

Fracture and Failure of Adhesives

Pascoe, John Alan

DOI

[10.1016/B978-0-12-822944-6.00042-6](https://doi.org/10.1016/B978-0-12-822944-6.00042-6)

Publication date

2023

Document Version

Final published version

Published in

Comprehensive Structural Integrity

Citation (APA)

Pascoe, J. A. (2023). Fracture and Failure of Adhesives. In *Comprehensive Structural Integrity* (pp. V7-2-V7-23). Elsevier. <https://doi.org/10.1016/B978-0-12-822944-6.00042-6>

Important note

To cite this publication, please use the final published version (if applicable). Please check the document version above.

Copyright

Other than for strictly personal use, it is not permitted to download, forward or distribute the text or part of it, without the consent of the author(s) and/or copyright holder(s), unless the work is under an open content license such as Creative Commons.

Takedown policy

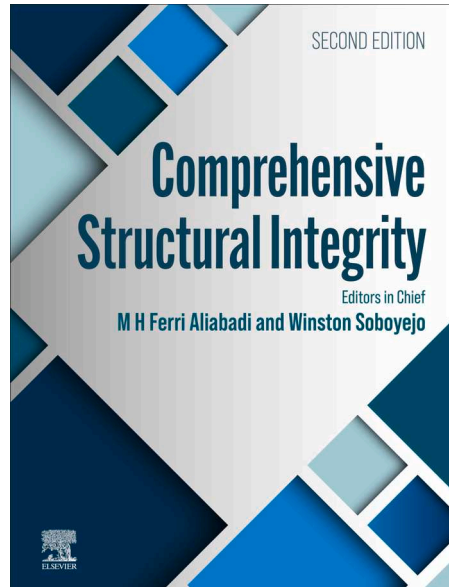
Please contact us and provide details if you believe this document breaches copyrights. We will remove access to the work immediately and investigate your claim.

Green Open Access added to TU Delft Institutional Repository

'You share, we take care!' - Taverne project

<https://www.openaccess.nl/en/you-share-we-take-care>

Otherwise as indicated in the copyright section: the publisher is the copyright holder of this work and the author uses the Dutch legislation to make this work public.



All other uses, reproduction and distribution, including without limitation, commercial reprints, selling or licensing copies or access, or posting on open internet sites, your personal or institution's website or repository, are prohibited.

For exceptions, permission may be sought for such use through Elsevier's permissions site at:

<https://www.elsevier.com/about/policies/copyright/permissions>

Pascoe, John-Alan (2023) Fracture and Failure of Adhesives. In: Aliabadi, Ferri M H and Soboyejo, Winston (eds.) *Comprehensive Structural Integrity, 2nd Edition*, vol. 7, pp. 2–23. Oxford: Elsevier.

<http://dx.doi.org/10.1016/B978-0-12-822944-6.00042-6>

© 2023 Elsevier Ltd All rights reserved.

Fracture and Failure of Adhesives

John-Alan Pascoe, Structural Integrity & Composites Group, Faculty of Aerospace Engineering, Delft University of Technology, Delft, The Netherlands

© 2023 Elsevier Ltd All rights reserved.

Introduction	4
Nomenclature	4
Stress Analysis	5
Volkersen's Analysis	5
Improved Analytical Methods	6
Finite Element Analysis	8
Designing for Improved Joint Strength	8
Failure Criteria	9
Continuum Mechanics	9
Elastic-Plastic Analysis	10
Fracture Mechanics	10
Accuracy	11
Failure Analysis	11
Failure Modes	11
Influence of Production	12
Case Study: Failure Analysis and Influence of Manufacturing	13
Effect of Thickness	13
Durability	14
Effect of Environment	15
Creep	15
Fatigue	16
Total life models	16
Strength and stiffness wear-out	17
Fracture mechanics models	17
Variable amplitude fatigue	18
Testing of Adhesive Bonds	18
Summary and Conclusion	19
Highlights	20
References	20

Abstract

This article presents an overview of methods for analyzing the fracture and failure of adhesives. Special attention is given to stress analysis in adhesive bonds, as the difficulty of performing an accurate stress analysis is a major limitation of many failure analysis methods. The article also covers the effect of manufacturing and operational environment, as well as long-term durability issues such as creep and fatigue.

Nomenclature

- A Fatigue based fracture toughness parameter (J mm^{-2})
- a Crack length (mm)
- b Width (mm)
- C Coefficient in the crack growth equation (-)
- E Young's modulus (MPa)
- G Shear modulus (MPa)
- G Strain energy release rate (J mm^{-2})
- J J-integral (J mm^{-2})
- l Overlap length (mm)
- m Exponent in the power-law fracture criterion (-)
- N_f Number of load cycles until failure (-)
- n Number of load cycles (-)

n	Exponent in the power-law fracture criterion (-)
n	Exponent in the crack growth equation (-)
P	Force (N)
R	Stress ratio (-)
S_a	Stress amplitude (MPa)
S_{max}	Maximum stress (MPa)
S_{min}	Minimum stress (MPa)
S_R	Residual strength (MPa)
S_u	Ultimate tensile strength (MPa)
t	Thickness (mm)
x	x-coordinate (mm)
κ	Crack growth similitude parameter (-)
κ	Strength degradation parameter (-)
σ	Normal stress (MPa)
τ	Shear stress (MPa)

Subscripts

adh	Adhesive
avg	Average
c	Critical
dry	Under dry conditions
max	Maximum
min	Minimum
thr	Threshold
wet	Under saturated conditions
yield	Yield strength
1,2	Referring to adherend 1, 2

Glossary

Adhesive failure A failure of the adhesion mechanism between the adhesive and one or both adherends.

Adherend A part that is joined to another part by means of an adhesive bond.

Cohesive failure A failure of the cohesion holding the material itself together.

Durability The ability of a bond to maintain structural integrity for the entire operational life.

Fatigue Gradual degradation and eventual failure of material due to the application of fluctuating load cycles below the quasi-static strength of the material.

Peel stress Normal stress in thickness direction of the adhesive.

Secondary bending Bending induced by misalignment of applied axial loads.

Similitude parameter Parameter that allows the comparison of two different situations (e.g., two different experiments, or an experiment and an in-service condition) on the basis that the same material behavior is expected when the similitude parameter is the same in both cases. As an example: a test coupon and a member of a truss structure are expected to fail when the normal stress in the part reaches the same value, even though the geometry and applied force will be very different. The normal stress acts as a similitude parameter here.

Key Points

- Provide an introduction to failure analysis of adhesive joints.
- Introduce the most common analysis methods for assessing the strength and durability of adhesive joints.
- Discuss the influence of manufacturing quality and environment on joint strength.
- Provide an entry point into the literature on fracture and failure of adhesive joints.

Introduction

The use of adhesives to join two parts of a structure together is a very old technology. There is evidence that birch bark tar was already used to join wooden hafts to stone tools some 200,000 years ago (Mazza *et al.*, 2006; Wadley *et al.*, 2009). By 40,000 years ago humans were already creating adhesive systems by mixing plant resins and ocher (Ambrose, 1998; Wadley *et al.*, 2009). In the present day, adhesive bonding is used across a wide variety of engineering fields, ranging from construction to packaging and from aerospace to biomedical engineering. Understanding and preventing failure of adhesives is therefore critical to ensuring structural integrity.

When it comes to analyzing the failure of adhesives, there are some differences compared to the analysis of other engineering materials. These are mainly related to how adhesives are applied. Typically, we are not so much interested how adhesives behave as a material by themselves. Instead, we are interested in how they behave when they are incorporated in an adhesive bond. In an adhesive bond, the adhesive layer is typically thin (certainly relative to the rest of the structure) and sandwiched between two parts with a higher stiffness. This creates a high degree of constraint in the adhesive, which may change its mechanical behavior compared to that of the bulk material (Kinloch and Shaw, 1981). Furthermore, the load transfer which occurs in an adhesively bonded joint can create stress concentrations and complex stress distributions, which means the strength of the joint cannot be properly evaluated by simply computing the average stress. Since most adhesives are polymers, the reader is referred to chapters 2.07 and 7.16 for more information on the bulk material behavior.

Many classes of adhesives exist, with a wide range of different properties, see e.g., (Brockmann *et al.*, 2009; Ebnesajjad, 2008; Pethrick, 2015; Sancaktar, 2018). In general these are polymeric materials that undergo some kind of curing reaction to reach their final state. This can occur spontaneously, e.g., after mixing the components of a two-component adhesive, or can be triggered by an external input, such as moisture, heat, or UV radiation.

This article will focus on methods for analyzing the structural integrity and failure of adhesive bonds, regardless of the specific adhesive that is selected. It should however be noted that specific test and analysis methods may only be suitable for specific classes of adhesive, for example depending on their (lack of) ductility or stiffness. This article will open with a section on the stress distribution in adhesive joints, followed by a discussion on different effects that can influence the joint strength. Next, the available failure criteria will be discussed. The article will then present how to analyze creep and fatigue, two phenomena that are crucial for understanding the durability of the bond. Finally a brief conclusion will summarize the article.

Nomenclature

To aid in communication, let us first define some basic nomenclature. In an adhesive joint, two pieces of material are being joined by bonding them with a third piece of material. The two pieces that are being joined are known as the adherends, while the material that is used to join them is the adhesive. Note that the two adherends do not need to be the same; they can be made of different materials and can have different shapes and dimensions. Fig. 1 illustrates some further nomenclature, including the shear modulus and thickness of the adhesive (G_{adh} and t_{adh} , respectively), the Young's moduli and thickness of the adherends: $E_{1,2}$, and $t_{1,2}$ and the joint width b and overlap length l . In the example of Fig. 1, the joint is being loaded by an axial load P . Fig. 1 also shows some basic joint designs. More advanced designs can be found in a variety of handbooks, e.g., (Adams *et al.*, 1997; Brockmann *et al.*, 2009; Ebnesajjad, 2008). In the context of adhesive bonds, tensile stresses out of the plane in which the adhesive is applied, are commonly referred to as peel stresses.

Typically, the resistance of adhesives to shear loading is much higher than their resistance to peel stresses (i.e., tensile loading) (Ebnesajjad, 2008). Therefore, adhesive joints should be designed such that the load transfer through the adhesive occurs as much as possible via shear stresses. This means that the plain butt joint design is to be avoided if at all possible. Additionally,

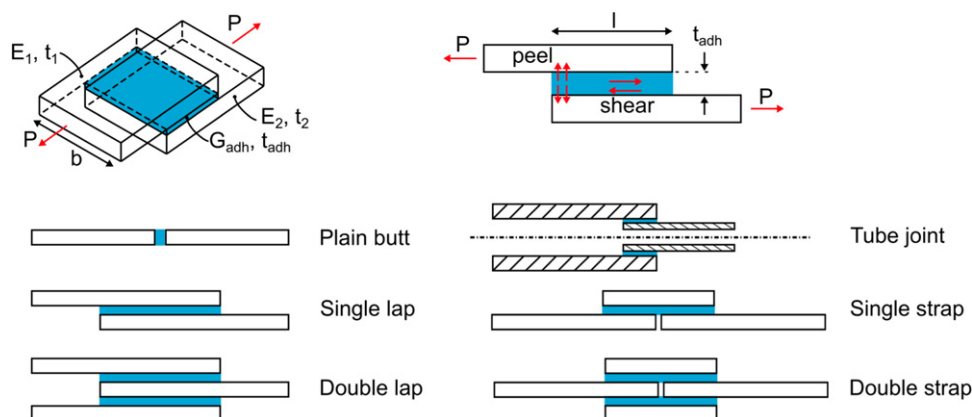


Fig. 1 Basic joint nomenclature and designs.

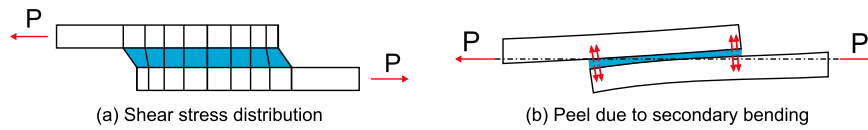


Fig. 2 Deformation of a single lap joint due to an axial load.

symmetrical joint designs such as the double lap, double strap, and tube joints are to be preferred to the single lap and single strap designs. This is because the eccentricity of the applied load in asymmetrical designs induces secondary bending, as illustrated in [Fig. 2\(b\)](#).

Stress Analysis

The most straightforward stress analysis for a single lap joint is to calculate the average shear stress τ_{avg} as:

$$\tau_{avg} = \frac{P}{bl} \quad (1)$$

with P representing the applied force and the width b and overlap length l defined according to [Fig. 1](#).

However, it is important to realize that this value is only a rough approximation for the stress distribution in the joint. In reality the stress distribution will be non-uniform, with large stress peaks near the ends of the overlap. Consequently, uncritical use of the average shear stress can lead to wrong conclusions. In general, average shear stress values should only be used to compare the performance of two joints that are identical in terms of geometry (especially overlap length) and adherend materials.

To start with the more detailed stress analysis, let us build up a qualitative understanding of the stress distribution in an adhesive joint. For this, consider how a single lap joint will deform when an axial tension is applied, as shown in [Fig. 2](#). There are two important effects. Firstly, at the free end of each adherend, there will be no strain, while at the opposite adhered, the strain will reach its maximum value at the same location. This implies there must be a peak shear stress in the adhesive ([Fig. 2\(a\)](#)). On the other hand, in the center of the overlap, the strain in both adherends will be equal, implying a low shear stress in the adhesive. Secondly, because the loads at either end of the joint are not co-linear, there will be secondary bending in the joint, as the joint tries to align the applied loads. This secondary bending induces transverse peel stresses, which are highest at the ends of the overlap ([Fig. 2\(b\)](#)). Combined, these two effects create a complex, multiaxial, stress distribution, which cannot be well described by only the average stress.

Volkersen's Analysis

An analytical solution for the shear stress distribution in the adhesive in a single lap joint was first developed by [Volkersen \(1938\)](#). Volkersen's approach is based on the shear lag principle, and requires the following assumptions:

- Peel stresses are neglected;
- The adhesive stresses are assumed to be constant across the thickness of the adhesive;
- The adherends are assumed to only deform in tension.
- The analysis is linear elastic.

These assumptions are clearly non-physical. Firstly, in reality, secondary bending will induce peel stresses (as mentioned above). This point is more relevant for asymmetrical geometries, than for symmetrical ones. Secondly, the stresses in the adhesive will not be constant through the thickness, even for thin bondlines, although it is of course especially noticeable for thick adhesives ([Gleich et al., 2001](#)). Thirdly, the adherends will not only deform in tension, but also in bending and shear ([Crocombe and Ashcroft, 2008](#)). This not only applies longitudinally; the difference in Poisson contraction will also result in the development of transverse stresses ([Adams and Peppiatt, 1973](#)). Fourthly, many adhesives and adherends are capable of plastic deformations. Despite these limitations, Volkersen's analysis can still illuminate some key points regarding the stress distribution in a joint, and how this depends on the geometry and adherend properties. It also has the advantage of being the most simple of the available analytical methods, apart from the use of the average shear stress ([Eq. 1](#)) of course.

As Volkersen's analysis forms the basis for the analytical approaches to stress analysis, many authors have presented equations for the shear stress distribution derived with Volkersen's method, see e.g., ([Adams et al., 1997](#); [Akhavan-Safar et al., 2021](#); [Crocombe and Ashcroft, 2008](#); [Klein, 1997](#); [Tong and Luo, 2018](#)). These equations take different forms, depending on the chosen coordinate system ($x = 0$ can represent either the end of the overlap, or the middle of the overlap), and whether the adherends are assumed to be made of the same material. Thus, different equations are presented by different authors. Here, we will use the form presented by [Crocombe and Ashcroft \(2008\)](#). For this equation both adherends are made of the same material ($E_1 = E_2$), but the thicknesses (t_1 and t_2) can be different. The x -coordinate has its origin ($x = 0$) at the center of the overlap, and is normalized by the overlap length to give $X = x/l$. The equation then takes the form ([Crocombe and Ashcroft, 2008](#)):

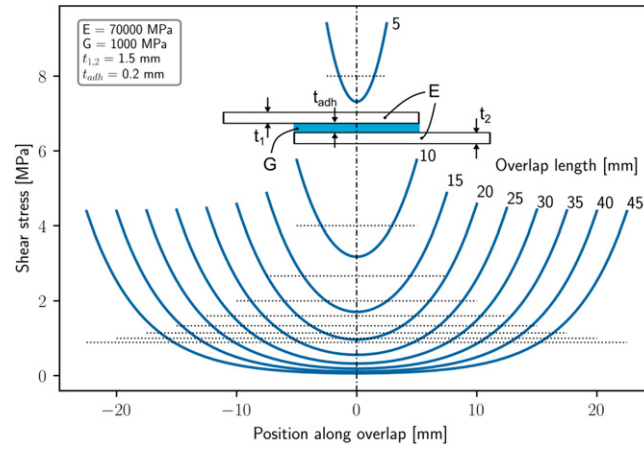


Fig. 3 Shear stress distribution for different overlap lengths, according to Volkersen's method (Eq. 2). The dotted lines indicate the average shear stress.

$$\tau = \tau_{avg} \left[\frac{\omega \cosh \omega X}{2 \sinh \frac{\omega}{2}} + \left(\frac{t_1 - t_2}{t_1 + t_2} \right) \frac{\omega \sinh \omega X}{2 \cosh \frac{\omega}{2}} \right] \quad (2)$$

with τ_{avg} given by Eq. 1 and the parameter ω equal to:

$$\omega = \left(1 + \frac{t_1}{t_2} \right) \frac{Gt_2^2}{Et_1 t_{adh}} \quad (3)$$

The peak stresses occur at the joint ends ($X = \pm 0.5$). The lowest stresses will occur for the case that the substrates are identical ($t_1 = t_2 = t$), in which case we can write (Crocombe and Ashcroft, 2008):

$$\frac{\tau}{\tau_{avg}} = \frac{\omega}{2} = \sqrt{\frac{Gt_2^2}{2Et_1 t_{adh}}} \quad (4)$$

Fig. 3 shows the shear stress distribution at different overlap lengths according to Eq. 2, for the material properties shown in the figure. The dotted lines indicate the average shear stress. It is clear that the peak shear stress at the ends of the overlap is much higher than the average shear stress.

Despite the simplifications in Volkersen's method, Eq. 3 and Fig. 3 can still illustrate some important points. First of all, the average shear stress decreases as the overlap length is increased, while the peak stress is more or less constant once the overlap length reaches 25 mm. This is important to realize, because this peak stress will be what triggers failure of the joint. If one characterizes the stress in the joint by calculating the average stress, this would give the impression that increasing the overlap length would improve the joint strength. However, after a relatively short length, further increases of overlap length no longer increase the joint strength, because there is no decrease of the peak stress. It should be noted that this consideration applies in particular to the static strength of the joint for a brittle adhesive. A long overlap length may still be desirable to improve resistance to creep (because a large part of the adhesive will only be lightly loaded), or to provide a buffer to increase durability and damage tolerance (Potter, 1979).

Based on Eq. 4 we can further observe that the peak shear stress will increase for higher adhesive shear modulus but decrease for higher adherend stiffness, i.e., increasing either the adherend modulus or the adherend thickness will decrease the peak adhesive stress (the stiffness of the adherend is given by the product Et). Klein (1997) presents an analysis based on Volkersen's method, but where the adherend moduli and thicknesses are allowed to be unequal. In that case the stress distribution is no longer symmetrical about the middle of the overlap. Instead, the peak stress will be increased at the side of the more flexible adherend, and decreased at the side of the stiffer adherend. The exact peak stress values will of course depend on the ratio of adherend stiffnesses.

Note that Eq. 4 predicts that the peak stress will be lower if the adhesive thickness is increased. This would imply that increasing the adhesive thickness results in a higher joint strength. However, in practice the opposite is seen: higher thickness leads to lower strength (Adams et al., 1997). Various explanations have been proposed for this, which will be discussed at a later point in the article.

Improved Analytical Methods

The assumptions in Volkersen's method are quite limiting, so to get a more accurate prediction of the stress distribution, a more detailed analysis is needed. Over the years many more analytical methods have been developed, addressing the various assumptions that limit Volkersen's method. While these analyses are more accurate, they are also more complex, and (like Volkersen's method itself) typically are only applicable to relatively simple geometries, such as single or double lap joints. In

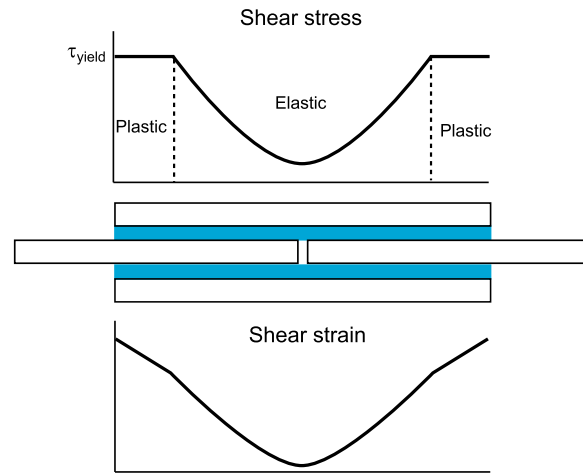


Fig. 4 Schematic illustration of the stress and strain distribution for an elasto-plastic adhesive.

practice, one should therefore consider whether it is worthwhile to employ these analytical methods, or if it is better to immediately choose to perform a finite element analysis.

Goland and Reissner (1944) were the first to improve on Volkersen's method. The Goland and Reissner approach takes into account the rotation of the adherends, and thereby also calculates the peel stresses. This approach to calculating the stress distribution was then further improved in (Hart-Smith, 1973a,b), which also included the effect of adhesive plasticity. Hart-Smith's work formed an important component of the Primary Adhesively Bonded Structure Technology (PABST) program. One of the outcomes of this program was a design handbook for adhesive bonding, which contains many practical guidelines for design of adhesive bonds from an aerospace industry perspective and is freely available online (Potter, 1979).

The Goland and Reissner approach still neglects shear deformation and the distribution of tensile stresses across the adherends. These points were addressed by in the model of Adams and Peppiatt (1973), which as previously mentioned, also includes the transverse stresses due to the Poisson contraction. Ojalvo and Eidinoff (1978) developed a model that could also take into account the variation of the shear stresses across the adhesive thickness. Bigwood and Crocombe (1989) generalized the Goland and Reissner analysis so it can be applied to single overlap configurations with an arbitrary end load. This also means the analysis can be applied to a range of different geometries, not just a single lap joint. In the same paper Bigwood and Crocombe also provide a set of simplified design formulae, which can be used for the case of similar adherends with long overlaps. Another important result from Bigwood and Crocombe (1989) is that the adhesive shear stress will induce a moment in the adherend (this follows from basic mechanics), which will reduce the shear stress. Consequently, the maximum stress predicted by the Volkersen equation is a factor two higher than that predicted by the Crocombe-Bigwood equations (Crocombe and Ashcroft, 2008). This matches with the experimental results presented in Adams *et al.* (1997, [Fig. 2]) showing that both the Volkersen and Goland and Reissner's models severely underestimate the failure load (at least for the adherend and adhesive properties shown in Adams *et al.* (1997)).

Cheng *et al.* (1991) built on the work of Goland and Reissner and Hart-Smith to create closed form solutions for a single lap joint where the adherends can have different thicknesses and lengths and can consist of different materials. A similarly general method was presented by Adams and Mallick (1992). This model has the advantage that it can also take into account elasto-plastic behavior of the adhesive. Unfortunately this comes at the cost of requiring a numerical solution, rather than providing closed-form expressions. At the time Adams and Mallick considered that finite element analysis required specialist knowledge and therefore their method still had advantages for industrial practice. Essentially they argued that their method was easier to implement, yet still agreed closely with finite element results, except right at the overlap edges. In the present day, finite element software has been widely adopted in industry, and finite element analysis is a standard part of engineering education (Akhavan-Safar *et al.*, 2021; Ashcroft and Mubashar, 2018). Therefore it can be questioned whether setting-up a numerical non-linear analysis rather than immediately opting for a finite element analysis is worthwhile (da Silva *et al.*, 2009b).

Most of the analyses described above assume elastic material behavior. In reality, many adhesives exhibit elastic-plastic behavior. This has been treated analytically by (Hart-Smith, 1981, 1973a,b) and also in the Adams and Mallick (1992) model. Hart-Smith's work was incorporated into the computer code A4EI (Hart-Smith, 1981), which is still the industry standard in the aerospace industry for analyzing the stress in bonded joints (Jones *et al.*, 2018).

Fig. 4 shows schematically the stress and strain distribution in a double overlap joint, based on Hart-Smith's elasto-plastic analysis, in which the adhesive is assumed to be perfectly plastic (Potter, 1979). It can be seen that the shear strain still shows a peak value at the edges of the overlap, but the shear stress is "cut off" at the yield strength τ_{yield} . This creates two plateau regions where the shear stress is constant, which are separated by a more lightly loaded elastic trough. According to Hart-Smith's analysis (Potter, 1979), if the adhesive is loaded up to the yield strength along the entire overlap, increasing the overlap length will increase the joint strength. Once the overlap length is long enough that the elastic trough is formed however, the joint strength remains constant, even if the overlap length is increased further.

This section has highlighted some of the key works on analytical methods for calculating the stress distribution in an adhesive joint, but does not provide an exhaustive overview. For a very detailed discussion of the stress distribution in an adhesive joint, including many finite element results, the reader is referred to [Adams *et al.* \(1997\)](#). For a more complete historical overview, [Akhavan-Safar *et al.* \(2021\)](#) have recently provided an excellent review. Further discussions and reviews of the available analytical methods can also be found in a variety of other reviews and handbooks, such as ([Crocombe and Ashcroft, 2008](#); [da Silva *et al.*, 2009a,b](#); [Gleich, 2002](#); [Ramalho *et al.*, 2020](#); [Tong and Luo, 2018](#); [Tserpes *et al.*, 2021](#)).

Finite Element Analysis

It has already been mentioned that analytical formulations that attempt to take into account the full complexity of the stress distribution in an adhesive bond become very complex, in some cases even requiring numerical solutions, e.g., ([Adams and Mallick, 1992](#)). Even then, these methods are usually still only formulated for relatively simple geometries, such as single or double overlap joints. To analyze more complex geometries that may be found in service, the use of a finite element analysis is therefore likely the most appropriate choice ([Adams, 1989](#)).

Finite element analyses furthermore have the advantage that they can accommodate not just traditional stress analysis, but also damage-based analysis ([Akhavan-Safar *et al.*, 2021](#)). This allows engineers to model the effect of defects created during manufacturing or sustained in service, providing evidence for setting acceptable damage limits. These damage-based analyses are typically performed by using cohesive zone modeling (CZM) or the extended finite element method (XFEM) to model the presence of damage in the model. Fracture mechanics based criteria are then used to identify when damage will propagate and lead to failure of the bond. Finite element analysis not only allows for modeling more complex joint lay-outs, but also the modeling of key details, such as the spew fillet at the end of the bond ([Adams and Peppiatt, 1974](#); [Crocombe and Adams, 1981](#); [Doru *et al.*, 2014](#); [Kemal Apalak and Davies, 1994](#)). This is an important detail to model, as it has been shown that the spew fillet will reduce the peak stresses at the overlap ends, thereby resulting in an increased bond strength.

A number of considerations should be kept in mind when setting up a finite element analysis of a bonded joint, on top of those that apply for any numerical analysis (e.g., correct selection of boundary conditions and mesh size). [Ashcroft and Mubashar \(2018\)](#) identify three key concerns: (1) the small adhesive layer thickness, (2) the material constitutive laws and (3) singularities at the adherend-adhesive interface. The small adhesive layer thickness can make it difficult to create a suitable mesh without having either an excessive number of elements, or having unacceptable element distortions. It should also be kept in mind that the adhesive stresses can vary across the thickness of the adhesive, and therefore it may be necessary to employ non-linear elements and/or to have multiple elements in thickness direction in the adhesive. The material constitutive law can be difficult because the adhesive material behavior can be complex (and difficult to characterize experimentally). On top of that, the adhesive material properties can be quite sensitive to environmental effects, which should be included in the analysis where relevant. When modeling the adherend-adhesive interface, theoretical singularities can arise, which do not correctly represent the physical behavior. In particular, these singularities could cause premature failure if for example a maximum stress or strain failure criterion is used. As a solution to this last point [Ashcroft and Mubashar \(2018\)](#) suggest using failure criteria that are for example based on average values over a certain region, or on all elements in a certain region exceeding the criterion, rather than just one. Alternatively, [Akhavan-Safar *et al.* \(2021\)](#) review the use of a critical generalized stress intensity factor criterion as a way of dealing with the singularity. As a final consideration it can be mentioned that one of the lessons learned from the PABST program ([Potter, 1979](#)) was the importance of conducting non-linear analyses to correctly understand the behavior of the adhesive joint. This of course applies not just to analytical methods, but also to finite element analyses. In particular non-linear material models should be used for the adhesive, but where applicable also for the adherends, as yielding of the adherends can have a significant effect on the stress distribution, and can even be the dominant failure mode in certain cases.

Designing for Improved Joint Strength

The stress analysis methods show that in a simple overlap joint there are large stress concentrations at the ends of the overlap. This reduces the joint efficiency, defined as the ratio of the joint strength to the strength of the adherends. Careful design can increase the joint efficiency, by reducing the stress concentrations. The general rules here are to reduce peel stresses by avoiding secondary bending, and to avoid sudden jumps in stiffness, e.g., by employing tapering. Tapering can be done either by externally tapering the adherends, or by creating a scarf joint, in which the outer envelope of the joint remains straight. Another option is the use of a stepped joint. In this case there are effectively multiple overlaps, with stress peaks at the end of each overlap. By distributing the stress peaks across multiple overlaps in this way, the average stress in the total bondline is increased and the individual peaks are reduced. As discussed above, spew fillets can also be instrumental in reducing the stress peaks at the overlap ends.

Some possible design solutions for the overall bond geometry are presented in [Fig. 5](#), and more can be found in the literature, e.g., ([Brockmann *et al.*, 2009](#); [da Silva *et al.*, 2018a](#); [da Silva and Campilho, 2015](#); [Ebnesajjad, 2008](#); [Kupski and Teixeira de Freitas, 2021](#); [Mallick, 2018](#); [Shang *et al.*, 2019](#)). These designs will produce a more efficient joint, but they come at the cost of increased manufacturing effort. When composite adherends are used, the design of the adherends themselves can also play an important role in the final joint strength and failure modes ([Kupski *et al.*, 2019](#); [Shang *et al.*, 2019](#)). More recently, researchers have been

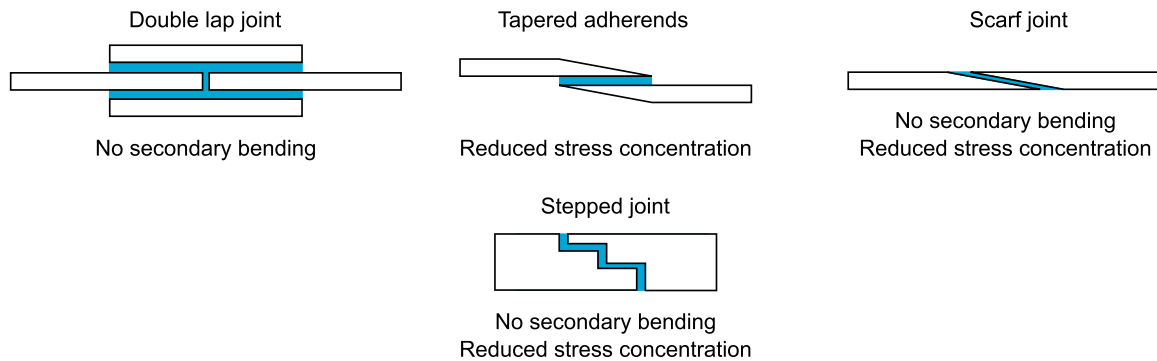


Fig. 5 Possible joints designs to reduce peak stresses.

developing features that can be inserted within the bondline to increase the bond strength. For example Minakuchi and co-workers (Hisada *et al.*, 2020; Minakuchi, 2015) have developed a crack arrestor based on interlocking fibers that are inserted into the bond line. Another example is the concept of inserting a spiked metal sheet in the bond line, as presented in Bisagni *et al.* (2018).

Within the aerospace industry, an important concern is the possibility of the growth of disbonds during the service life of an aircraft, which can be difficult to detect (Kruse, 2013; Kruse *et al.*, 2018). A number of researchers are therefore working on the development of joint features that can guarantee that a disbond will be arrested before reaching a critical size, thereby enabling the certification of bonds in primary (i.e., safety-critical) structures. These disbond arrest features can either rely purely on features that are inserted in the bondline (Steinmetz *et al.*, 2021) or they can make use of mechanical fasteners, that penetrate through the adherends (also called hybrid joints) (Chowdhury *et al.*, 2016).

Apart from adjusting the joint geometry, another approach is to tailor the adhesive properties. Ideally the adhesive should be flexible and ductile at the ends of the overlap, in order to reduce the peak stresses (recall Eq. 4). In the middle of the overlap a stiffer adhesive would be preferred, in order to carry more load in the lightly loaded part of the overlap. Because the load here is lower, a more brittle behavior can be accepted. da Silva and Lopes (2009) therefore developed a mixed-adhesive technique, where a flexible and ductile adhesive was applied to the overlap ends, and a brittle adhesive was used in the center of the overlap. Silicon rubber strips were used to separate the adhesives. The mixed-adhesive joint was shown to have a higher strength than joints that contained either of the individual adhesives over the full length. The use of mixed adhesives falls in the category of functionally graded adhesive joints. Durodola, (2017) provides a recent review that concludes that functionally graded adhesives have clear theoretical benefits, which have also been confirmed experimentally. The wide-spread adoption of functionally graded adhesives has however been limited by manufacturing challenges. Typically functionally grading involves the combination of two different adhesives, and so it can be challenging to find a surface pre-treatment that is suitable for both. Another challenge is creating and maintaining the right fractions and grading of the different adhesives at the desired locations, both during application of the adhesive and during the cure cycle. Stapleton *et al.* (2012) point out the additional concern that tailoring the functional grading for a certain load case may make the joint less effective at resisting other (potentially unexpected) load cases.

Failure Criteria

Prediction of the joint strength requires the use of a failure criterion. Different failure criteria are available, which match different analysis methods. Recent reviews of failure criteria have been provided by Tserpes *et al.* (2021) and Ramalho *et al.* (2020). Different categories of failure criteria can be distinguished, which include elastic and elasto-plastic continuum mechanics based methods and fracture mechanics based criteria.

Continuum Mechanics

Classical continuum mechanics failure criteria are based on the maximum stress or strain in the adhesive bond. Given the multiaxial stress state in an adhesive, a multiaxial criterion, such as the principal stress and strain (Adams *et al.*, 1997) or the von Mises criterion may be more appropriate (Tong and Luo, 2018). Stress based criteria are more suited for linear elastic analyses, whereas strain based criteria may be more suitable for nonlinear analyses (da Silva *et al.*, 2009b). Interestingly Adams *et al.* (1997) present a comparison of predictions and experimental data for four different adhesives. For two of these adhesives the maximum principal stress proves to give the best prediction of joint strength, while for the other two adhesives the maximum principal strain proves to be more accurate. Unfortunately, it is not clear if it could be determined a priori which criterion would be most accurate.

A difficulty with applying strength and strain based criteria is that they rely on accurate calculations of the peak stresses and strains, whereas the available analytical models have limited accuracy. In a finite element analysis on the other hand, there may be a stress/strain singularity at the adherend – adhesive interface, creating convergence issues and introducing a mesh dependency (Ramalho *et al.*, 2020). This has led to the adoption of criteria based on the theory of critical distances (Taylor, 2008), categorized

as process zone methods in (Tserpes *et al.*, 2021). In these theories, the critical parameter is not the maximum stress, but the average stress value in a point, line, area, or volume (depending on the precise method) at some critical distance from the stress singularity (Tserpes *et al.*, 2021). This for example allows the failure criterion to be compared to the strain on the adhesive mid-plane, avoiding the adherend/adhesive stress singularity, such as in the criterion proposed by Ayatollahi and Akhavan-Safar (2015).

Elastic-Plastic Analysis

In his elastic-plastic analysis Hart-Smith (1973a,b) proposed a critical adhesive strain energy density as the failure criterion. I.e., joint failure will occur when a critical strain energy density is reached in the adhesive. Jones *et al.* (1993) showed that the effect of creep during load holds should be accounted for when applying such a procedure. Chiu *et al.* (1994) demonstrated that for a double lap joint, the critical strain energy density could be calculated based on a purely elastic analysis. Recently, Jones *et al.* (2018) have shown this also applies for step lap joints, which means it is not required to know the precise shape of the adhesive stress-strain curve to apply the critical strain energy density criterion.

Another elastic-plastic criterion is the general yielding criterion proposed by Crocombe (1989). The concept behind this criterion is as follows: due to plastic deformation, adhesives exhibit a level of strain beyond which a further increase of strain will not increase the stress in the adhesive. Thus Crocombe argued that –as long as there is no local failure– joint failure will occur when all the adhesive material in the bond line reaches this level of strain. In other words, joint failure will occur when there is general yielding in the bond line. The bond strength can thus be determined by determining the load at which general yielding takes place. Crocombe already pointed out that this method is most suited for shear failure and is not a useful concept for cleavage type failure. In their comparison of analysis models, de Sousa *et al.* (2017) concluded that the general yielding criterion is accurate for “highly ductile adhesives” and “moderately ductile adhesives with short overlaps”, but was not suited for brittle adhesives. Similarly Gleich *et al.* (2001) criticized the general yielding criterion, on the basis that most joints fail due to local failure, especially in the case of brittle adhesives. This example illustrates the more general point that the ductility, or lack thereof, of the adhesive can determine which failure criteria are suitable.

Fracture Mechanics

Another category of failure criteria are those based on fracture mechanics. These are especially useful to analyze the effect of any defects or damages in the bond line (Dillard, 2021). Fracture mechanics failure criteria state that unstable crack growth will occur when the strain energy release rate (SERR, G), exceeds a critical value G_c , which is determined experimentally. In the case of a ductile adhesive, the J-integral may be used instead of the strain energy release rate (Sadeghi *et al.*, 2018). A downside of using fracture mechanics is that it can only be applied if there is some initial crack. When analyzing a new design, it may not be clear what crack length is reasonable to assume. One solution to this is to adopt a CZM analysis, in which a strength-based criterion (implicitly incorporated into the CZM formulation) takes care of the crack initiation (Dillard, 2021). In the aerospace industry the common practice is to define an initial crack based either on a statistical analysis of the manufacturing quality achieved in practice, or based on the detectability limits of a prescribed inspection technique.

The process of fracture in an adhesive bears much resemblance to the process of delamination in a fiber reinforced polymer composite. In both cases there is growth of a crack through a thin polymer layer. In fact, some structural adhesives are also used as matrix material for fiber reinforced composites. Although the two research communities are somewhat separate, when applying fracture mechanics methods to adhesive bonds, it can be fruitful to also consider the state-of-the-art for delamination of composites (Pascoe *et al.*, 2013a).

In a general load case, an adhesive bond will experience mixed-mode crack opening, and therefore a mixed-mode fracture criterion is needed. The most simple solution is to simply sum up all the different SERR components and compare this to the critical SERR value. This approach only works if the critical SERR value was measured for the same mode-mixity as the case being analyzed. A more flexible approach is to adopt a mixed-mode fracture criterion. One commonly used mixed-mode criterion is the power-law criterion (Wu and Reuter, 1965):

$$\left(\frac{G_I}{G_{Ic}}\right)^m + \left(\frac{G_{II}}{G_{IIc}}\right)^n = 1 \quad (5)$$

Different researchers have reported using different m and n values, e.g., (Jiang *et al.*, 2021; Tong and Luo, 2018; Zhang *et al.*, 2010), suggesting that these are material (and possibly adhesive thickness) dependent. Apart from the power law criterion, a variety of other mixed-mode criteria have been developed; for a recent review see the introduction of Jiang *et al.* (2021).

Use of a mixed-mode criterion requires partitioning the SERR into the separate mode components. This is not a straightforward matter. Williams (1988) provided a solution for a symmetrical problem, i.e., with the crack in the mid-plane and identical material on either side. However, this method produces inaccurate results in asymmetric conditions, such as in bi-material joints. For this case an alternative strain-based method was recently proposed by Arouche *et al.* (2021). A further review of different methods for partitioning the SERR modes can be found in Wang *et al.* (2021). This review also discusses different experimental methods for testing bi-material interfaces. Rather than relying on analytical mode partitioning, finite element methods, such as the virtual crack closure technique (VCCT) can provide accurate results (Arouche *et al.*, 2021). Apart from VCCT, fracture mechanics criteria can be

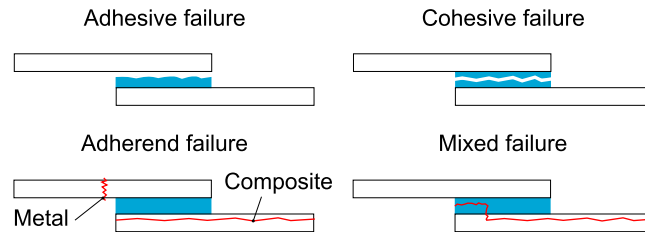


Fig. 6 Different failure modes in adhesive bonds.

incorporated into finite element analyses with various other numerical techniques such as the cohesive zone model (CZM) or extended finite element method (XFEM). For a review of these methods see (Tserpes *et al.*, 2021).

A further development of fracture mechanics is finite fracture mechanics (FFM), first proposed by Leguillon (2002). In FFM crack growth requires simultaneously satisfying two criteria, one based on stress and the other based on toughness / energy release. This was first applied to bonded joints by Leguillon *et al.* (2003), and further developments have been reviewed by Tserpes *et al.* (2021).

Accuracy

The performance of different strength prediction methods based has been compared by da Silva *et al.* (2009b) and de Sousa *et al.* (2017). Both works conclude that the accuracy of the different methods depends on the materials being examined. De Sousa *et al.* (2017) conclude that Volkersen's model only works for brittle adhesives and short overlaps, while the Goland and Reissner and Hart-Smith models underpredicted the joint strength for all adhesives and joint configurations. The Hart-Smith model was judged to be best for all adhesives. For the most accurate results however, de Sousa *et al.* recommend adopting a CZM analysis. In de Sousa's work, XFEM performed poorly, which was attributed to the mesh-dependence of the initiation criteria, and the inability of the initiation criteria to capture mode-mixity. Thus a reformulation of the XFEM with different initiation criteria might be expected to perform better. da Silva *et al.* (2009b) come to similar conclusions regarding the analytical models as de Sousa *et al.* Additionally, da Silva *et al.* conclude that predicting the strength of joints with long overlaps and brittle adhesives is difficult, but that linear analyses always give a safe prediction (i.e., the predicted strength is lower than the experimentally measured value). For joints with ductile adhesives and elastic adherends the Hart-Smith (1973a,b) model was found to give good predictions, although da Silva *et al.* recommend using a criterion that is only based on the shear stress, rather than on a combination of shear and peel. If the adherends exhibit yielding, then da Silva *et al.* recommend an adherend yielding based equation proposed in Adams *et al.* (1997).

Failure Analysis

Understanding failure of adhesive bonds course requires an understanding of the applied load and the resulting stress distribution in the adhesive. However, on top of that it is also important to understand the operating environment, as the bond strength can be sensitive to environmental factors, such as temperature, moisture, and other chemicals. Errors or defects during manufacturing can also have significant effects on bond strength and durability, resulting in unexpected in-service failures.

Failure Modes

Adhesive bonds can suffer from different failure modes, as illustrated in Fig. 6. When analyzing a failure by comparing two different experiments, or comparing an in-service failure to the design case, it is critical to ensure the failure modes are the same. If the failure modes are different, then also a different joint strength should be expected. An unexpected (change of) failure mode can point to incorrect design assumptions, manufacturing errors, or environmental influences. The failure modes can be categorized as follows:

- Adhesive failure is a failure of the adhesion between the adhesive and one of the adherends. In practice it can be diagnosed by the lack of adhesive residue on one of the fracture surfaces. Adhesion failure indicates a lack of chemical bonding, and the remedy is often to improve the surface preparation process prior to bonding. In the aerospace industry, adhesion failures are considered an unacceptable failure mode (Federal Aviation Administration, 2010). This means that if adhesive failure is found during development testing the part cannot be certified. Instead changes to the design and/or manufacturing process need to be made until only cohesive failure is found. As mentioned above, this likely means selecting or developing a more appropriate surface pre-treatment. Note that even if a suitable surface preparation process has been selected, contamination or other lapses of manufacturing quality can still result in adhesive failure in production parts. Therefore, proper environmental and process controls during manufacturing are crucial to avoiding adhesive failure.

- Cohesive failure is a failure due to lack of cohesion within the adhesive itself. It can be diagnosed by the presence of adhesive residue on both fracture surfaces. If the joint strength at which cohesive failure occurs is too low, a stronger adhesive needs to be selected, or the joint needs to be redesigned to reduce the (peak) adhesive stresses.
- In an adhesive joint there are not only stress concentrations in the adhesive, but also in the adherends, which can result in (cohesive) adherend failure. In metals this typically results in a transverse crack, but in laminated composites the transverse strength may be the weakest link, which results in delamination of the first ply adjacent to the bond line. Whether failure occurs in the adhesive or the adherend depends in part on the laminate stiffness and lay-up (Kupski *et al.*, 2019). An adherend failure mode indicates that the adhesive is not the weakest link in the structure, which is in principle desirable. However, it should be noted that the presence of stress concentrations mean that even if the failure mode occurs in the adherend, this does not imply a 100% joint efficiency (where the joint efficiency is the ratio of the joint strength to the strength of the structure remote from the joint). Depending on the design and operational context, an adherend failure mode could be preferable to a cohesive failure of the adhesive, if it is easier to detect by operators or maintenance technicians.
- Another failure mode that can in particular be observed for composite adherends is mixed failure, where the crack migrates from the adhesive into the composite adherend. In some cases the crack can also migrate back into the adhesive layer again. Goh *et al.* (2013) show an example of this in a scarf joint. Whether such crack migrations will occur, and at which locations, depends on the local stress state and the adherend lay-up (Kupski *et al.*, 2019). As a general guideline, a crack will find it more difficult to propagate through a ply in which the fibers are aligned along the crack-growth direction. Conversely, the crack will find it more easy to jump through a ply in which the fibers are perpendicular to the crack growth direction. This is because in the case of perpendicular fibers the crack can find a path between the fibers, without needing to break any of them.

Apart from the general failure modes described above, the specific failure initiation location can vary depending on the detailed geometry (e.g., in the case of a spew fillet) and the adherend properties. Adams *et al.* (1997) provide a very detailed demonstration of how the critical location for failure can depend on the adherend properties, and even on the applied load.

Influence of Production

Manufacturing quality is critical to obtaining the desired joint behavior. According to the Federal Aviation Administration: “Many bond failures and problems in service have been traced to invalid qualifications or insufficient quality control of production processes” (Federal Aviation Administration, 2010).

First of all an appropriate surface pre-treatment needs to be selected. This pre-treatment is specific for the combination of adherend and adhesive (Critchlow, 2018). Development of improved surface treatments is an active area of research, currently especially focusing on reducing the environmental impact of the surface treatment processes (Budhe *et al.*, 2017; Marques *et al.*, 2020; Matinlinna *et al.*, 2018; Park *et al.*, 2018; Yudhanto *et al.*, 2021).

The surface treatment can consist of multiple steps, which all have different functions. Depending on the specific case some functions may or may not be necessary. A proper surface treatment should firstly ensure there are no contaminants (e.g., grease, dirt, moisture) in the bond line, which would prevent good adhesion. For metal adherends, this can also involve removing oxide films. Secondly, it may be desirable to increase the surface roughness of the adherend, for example by grinding, abrading, or grit blasting. Increasing the surface roughness creates a larger effective surface area on which adhesion can take place. Furthermore, it increases the potential for mechanical interlocking between adhesive and adherend. Mechanical interlocking can also be improved by growing suitable microstructures at the adherend surface. This happens for example during chromic acid anodisation of aluminum. Thirdly, to maximize the bond strength, the adhesive should of course cover the entire overlap surface, i.e., a good wetting is required. The degree of wetting is influenced by the surface energy of the adherend, which should ideally be as low as possible. A suitable surface treatment can be used to modify this as needed. Apart from modifying the surface energy to improve wetting, the surface treatment can also be used to improve the chemical compatibility between the adherend and the adhesive, e.g., with a chemical coupling agent or bond primer (Mallick, 2018) to improve the bonding between the adhesive and the adherend. The discussion above has hopefully shown the importance of proper surface preparation. It should be clear that if any of the mentioned functions are impaired, this could strongly influence the bond strength, especially if it induces a switch of failure mode from cohesive to adhesive.

Once the surface is prepared, the adhesive needs to be applied. The application process will depend on the adhesive, which could be in a liquid, paste, or film form. Some adhesives consist of two components that need to be mixed before application. In that case ensuring both the correct component ratio, and a sufficient degree of mixing, is required to get the desired material properties. Some adhesive systems can undergo spontaneous curing reactions, and therefore require special storage conditions, or have limited shelf-lives, which should be respected. Many adhesives also have limited working lives once their packaging is opened, or once they are mixed, in which case it should be ensured that the adhesive is applied within this time-window. For the application, the key points are to ensure the correct coverage, without any dry spots (holidays), and the correct thickness, as the adhesive thickness can influence the bond strength. To control the thickness, a variety of techniques are available, such as including spacing wires in the bond line or mixing glass beads into the adhesive. Film adhesives may incorporate a carrier mat to help control the thickness. If adhesive squeeze-out is required to create a spew fillet, enough adhesive needs to be applied to make this possible.

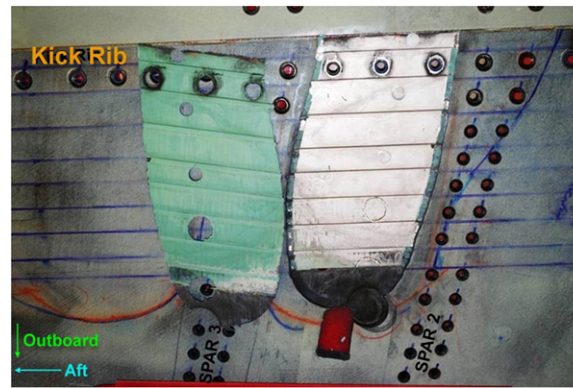


Fig. 7 The excised disbond. Note the lack of adhesive residue on one of the fracture surfaces, as indicated by the white color. Image from Mueller, E.M., Starnes, S., Strickland, N., Kenny, P., Williams, C., 2016. The detection, inspection, and failure analysis of a composite wing skin defect on a tactical aircraft. *Compos. Struct.* 145, 186–193. Available at: <https://doi.org/10.1016/j.compstruct.2016.02.046>. Reproduced with permission from Elsevier.

After application of the adhesive it needs to be cured. Curing requires different things, depending on the adhesive. Some adhesives cure by reacting with moisture in the air, or need exposure to UV radiation to activate the curing reaction. Two-component adhesives may undergo a spontaneous reaction once mixed, requiring no further input, although elevated temperatures can be used to speed up the curing process. Other systems require the elevated temperature not just to speed the curing process, but to cure correctly in the first place. In this case it is also important to consider heat transfer and the thermal inertia of the adherends and any jigs or tooling, to ensure all parts of the adhesive reach the required temperature for the required length of time. In many cases pressure should be applied during the curing of the adhesive. Firstly, this helps to increase the wetting by inducing flow of the adhesive. Secondly it can help prevent the formation of porosity or voids. For a more detailed discussion on curing, see (Pethrick, 2015). If the curing process is not carried out correctly, the adhesive will not reach the desired degree of cure, in which case its properties (e.g., strength, stiffness) will not be as expected.

Case Study: Failure Analysis and Influence of Manufacturing

A nice case study of a failure analysis and the influence of manufacturing is given in Mueller *et al.* (2016). Mueller *et al.* present an investigation into large disbonds that were detected in service in a titanium to carbon fiber / epoxy step lap joint in a fighter aircraft wing. Previously a study had been conducted on this joint by full-scale testing of specimens cut from retired wings (i.e., parts that had been subjected to in-service loads for a considerable life-time of usage) (Seneviratne *et al.*, 2015). In that study, the observed failure modes were either cohesive failure in the adhesive, or adherend failure, which were both the desired failure modes.

Nevertheless, ultrasonic inspection revealed the presence of large disbonds in the wing joint of specific aircraft in service, prompting the investigation of Mueller *et al.* (2016). In this investigation, the wing was removed from the aircraft and the damage was excised to allow for more detailed inspection. Notwithstanding the results of Seneviratne *et al.* (2015), it was already noticed at the macroscale that adhesive residue was present on only one of the fracture surfaces, indicative of adhesive failure, as shown in Fig. 7. A micrographic cross-section (shown in Fig. 8) confirmed that the crack ran along the titanium – adhesive interface, so this was indeed a case of adhesive failure. Further analysis showed the presence of titanium oxides containing high levels of fluorine. First the operating environment was analyzed, and no possible sources of fluorine could be identified. However, an examination of the manufacturing process showed that cleaning with a fluorine-containing acid solution was one of the pre-treatment steps, after which the part was to be cleaned with deionized water for several minutes. The investigation therefore concluded that insufficient rinsing lead to fluorine remaining present at the adherend surface, resulting in a decreased durability of the adhesion. This lead to the observed adhesive failures.

This case study illustrates a number of important points. In terms of the failure analysis, it demonstrates the value of collecting data at different length scales, and the importance of examining the manufacturing and operational contexts as well as the joint design and loading, to fully understand the failure. The case also illustrates that even if a suitable manufacturing process is selected (as shown by the positive results in Seneviratne *et al.* (2015), deficiencies in the execution of that process can lead to incidental failures in service.

Effect of Thickness

It is clear that the bond line thickness affects the joint strength, but predicting this effect is not so straightforward. Many of the analytical stress analysis methods contain the adhesive thickness as an input variable, see e.g., Eq. 4 or Akhavan-Safar *et al.* (2021). Typically these predict that for thicker adhesives, the peak stress should decrease, which would result in an increased joint strength

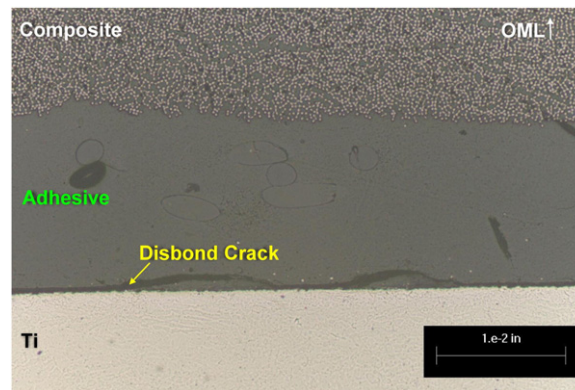


Fig. 8 Micrographic cross-section showing the location of the crack. Image from Mueller, E.M., Starnes, S., Strickland, N., Kenny, P., Williams, C., 2016. The detection, inspection, and failure analysis of a composite wing skin defect on a tactical aircraft. *Compos. Struct.* 145, 186–193. Available at: <https://doi.org/10.1016/j.compstruct.2016.02.046>. Reproduced with permission from Elsevier.

(Adams *et al.*, 1997). However, this hypothesis is not in agreement with experimental results, which show a decrease of joint strength as the adhesive thickness is increased (Adams *et al.*, 1997; Akhavan-Safar *et al.*, 2021).

Adams and Peppiatt (1974) attributed the decrease in bond strength for increased thickness to an increase of porosity or micro-cracking for thicker bond lines. This has proven difficult to validate experimentally. Bigwood and Crocombe (1990) and Crocombe (1989) pointed out the importance of performing a non-linear analysis and attributed the decrease in strength to faster spreading of yielding in thicker adhesive layers, resulting in global yielding at lower applied loads. da Silva *et al.* (2006) and Gleich *et al.* (2001) instead captured the effect of adhesive thickness by modeling the interface stresses at the adhesive/adherend interface. More recently Akhavan-Safar *et al.* (2017) successfully predicted the effect of thickness on bond strength based on a finite element method calculation of the longitudinal strain at the adhesive mid-plane. In short, Adams and Peppiatt attribute the thickness effect to a degradation on the adhesive properties, while the other authors point to an effect of the adhesive thickness on the adhesive stress distribution.

From the point of view of fracture mechanics, the bond line thickness has been found to affect the fracture toughness. Kinloch and Shaw (1981) found that there was an optimum thickness at which the toughness is maximized, with both lower and higher adhesive thickness resulting in lower toughness values. They explained this based on the effect of constraint on the plastic zone ahead of the crack tip. The plastic zone acts to shield the crack tip and dissipate energy, which is then not available for crack growth. This results in a higher (apparent) fracture toughness, as more energy is effectively required to grow the crack. According to Kinloch and Shaw, if the bond line thickness is lower than the optimum thickness, the plastic zone cannot fully develop, and hence the fracture toughness is reduced. On the other hand, if the thickness is too large, the plastic zone will develop in a more vertical orientation, and not extend as far ahead of the crack tip, again resulting in a lower fracture toughness. The optimal thickness will of course depend on the adhesive, but for structural adhesives is typically below 1 mm. More recently, Yan *et al.* (2001) have proposed that the decrease of fracture toughness at higher thicknesses is due to crack tip blunting and increased void coalescence. Pardoen *et al.* (2005) have pointed out that the length-scales at which the fracture mechanisms occur can be roughly comparable to the adhesive thickness (for thin adhesive layers, i.e., 100–200 μm). Therefore the constraint might affect not only the plastic zone, but also the fracture mechanisms themselves.

As one might expect, the bond line thickness will also affect the fatigue crack growth rate, as has been reviewed in (Azari *et al.*, 2011; Pascoe *et al.*, 2020). In their review Pascoe *et al.* (2020) identify that in general higher adhesive thickness is reported to result in lower fatigue crack growth rate and higher fracture toughness. However, this result is not uniform, and may depend on whether the thicknesses studied were above or below (or on either side of) the optimum thickness. In their own experiments, which involved three different thicknesses of an epoxy adhesive joining two aluminum adherends, Pascoe *et al.* found an increased crack growth rate at higher thicknesses, which they attributed to more energy being available for crack growth in the thicker adhesive.

Given the potentially significant effect of the bond line thickness on the joint strength, proper thickness control during manufacturing is important to ensure that production parts have the strength prescribed by the design. As has been mentioned in the section on manufacturing, this can be achieved through a variety of techniques. For an accurate analysis, if the bond-line thickness is not constant, this should be taken into account, although it will of course add complexity to the analysis.

Durability

The preceding models focus mainly on the response of an adhesive bond to a single application of load. However, depending on the application, the desired service life of adhesive bonds may be measured in decades or perhaps even centuries. In that case it is important to analyze the long-term performance of the bond, i.e., its durability. Key factors to consider here are the effect of the environment on the bond, its response to creep, and the fatigue behavior of the bond.

Effect of Environment

The properties of an adhesive bond are strongly dependent on the environment. The two aspects usually investigated are temperature and moisture, but if the adhesive may be exposed to other chemicals (e.g., hydraulic or de-icing fluids) their effect should be investigated as well.

The mechanical properties of the adhesive may be sensitive to the temperature, especially for adhesives which exhibit a glass transition. The effect on fatigue crack growth behavior has been reviewed in [Usman *et al.* \(2018\)](#). They report that in general an increased growth rate is observed at higher temperatures, but that non-monotonous behavior is sometimes seen, especially at the upper and lower ends of the tested temperature ranges. Usman *et al.* themselves conducted fatigue crack growth experiments on an epoxy adhesive in the range -55 – 80°C and found an increased crack growth rate as the temperature increased.

Apart from the effect on material properties, differences in thermal expansion coefficient between the adhesive and the adherends (or mutually between two dissimilar adherends) can result in thermal stresses which could give the appearance of a reduced joint strength. Note that for adhesives that cure at elevated temperatures, thermal stresses can be induced during the subsequent cooling to room temperature, and these will remain present in the structure. Thermal stresses can in principle be modeled by imposing the appropriate thermal strains, which depend on the temperature change and the coefficients of thermal expansion. The suitability of the chosen failure criterion should be checked in this case. The change in material properties as a function of temperature will require experimental characterization unless prior data is available.

A more long-term concern is the effect of moisture, which can diffuse into a bond over time-spans that can be in the order of years ([Pethrick, 2015](#)). When deliberately conditioning specimens at high relative humidity levels, initially a fast drop of bond strength is seen, which eventually levels off at 40%–60% below the original strength ([Ashcroft *et al.*, 2018](#); [Comyn, 2021](#)). It should be noted that moisture can attack not only the adhesive itself, but also the adherend-adhesive interface, with the consequence that a joint that fails cohesively under dry conditions, fails adhesively if it absorbs too much moisture ([Borges *et al.*, 2021](#)). In design, the effect of moisture can be accounted for by developing suitable knock-down factors for the strength, based on coupon testing. Aside from causing degradation of the material properties, moisture absorption by the adhesive can also result in swelling of the adhesive, which can lead to swelling stresses. Because there is usually a gradient of moisture concentration along the bond length (due to the slow speed of moisture diffusion) these swelling stresses will also be non-uniform. Therefore, [Akhavan-Safar *et al.* \(2021\)](#) state that a finite element analysis is required to correctly account for these stresses. This also requires obtaining an experimental coefficient of swelling.

A closed-form model to analyze the effect of moisture absorption has been presented by [Crocombe \(2008\)](#), based on the global yielding criterion. In this model the shear strength depends on the local moisture content, which is a function of both location and time. The shear strength varies linearly from a value of τ_{dry} (no moisture present) to τ_{wet} (saturated moisture concentration) and the moisture concentration is calculated via a Fickian diffusion model. The final bond strength is then calculated by integrating the local shear strength values along the length of the bondline.

Proper investigation of the effect of the environment still requires experimental testing, and it is thus important that material data is generated for temperatures, humidity levels, and moisture saturation levels that are properly representative of the operating environment. It should however be noted that [Ashcroft *et al.* \(2001\)](#) found that the results of accelerating aging tests do not necessarily correlate with the effects of natural aging. Properly accounting for aging effects therefore remains somewhat of an open question. For a further discussion of environmental effects, the reader is referred to the reviews in ([Adams *et al.*, 1997](#); [Ashcroft *et al.*, 2018](#); [Comyn, 2021](#)).

Creep

Given the viscoelastic nature of many adhesives, the creep behavior is an important durability concern if the joint is expected to carry static loads for long periods of time. According to [Adams *et al.* \(1997\)](#) creep is mainly a concern in cases of high stresses and temperatures close to (or exceeding) the glass transition temperature. Nevertheless, more recent experiments ([Geiss and Vogt, 2005](#); [Kasper *et al.*, 2021](#); [Khabazaghdam *et al.*, 2021](#); [Poulis *et al.*, 2020](#)) have reported creep even at room temperature. Crack growth under static external loading has also been observed ([Pascoe *et al.*, 2018](#); [Plausinis and Spelt, 1995](#)).

For the modeling of creep behavior, generic visco-elastic material models are available ([Geiß and Schumann, 2018](#)) and some work has also been done on models specifically for adhesive bonds, as reviewed in [Chen and Smith \(2020\)](#). Experiments to characterize the creep behavior are still needed. These experiments can be accelerated by using the time-temperature superposition principle. In this case creep tests are performed at different elevated temperatures, where creep is more rapid. This data can then be used to construct a master curve to predict the creep behavior at room temperature ([Geiß and Schumann, 2018](#); [Marques *et al.*, 2017](#)).

In terms of designing against creep, the design guidelines developed during the PABST program ([Potter, 1979](#)) emphasize the importance of the “elastic trough” in the center of the bond line ([Fig. 4](#)). Even if no yielding occurs, if the overlap is long enough, there will be a lightly loaded region in the center of the bond line ([Fig. 3](#)). The low loads in this region ensure that no creep will occur there. [Potter \(1979\)](#) also points out that as long as the adherend does not yield at the overlap ends, the deformation of the adherend will provide an upper bound on the adhesive strain. Furthermore, upon unloading, residual stresses are induced within the adherend which can recover the adhesive creep again, which prevents creep damage from accumulating. In short, although the

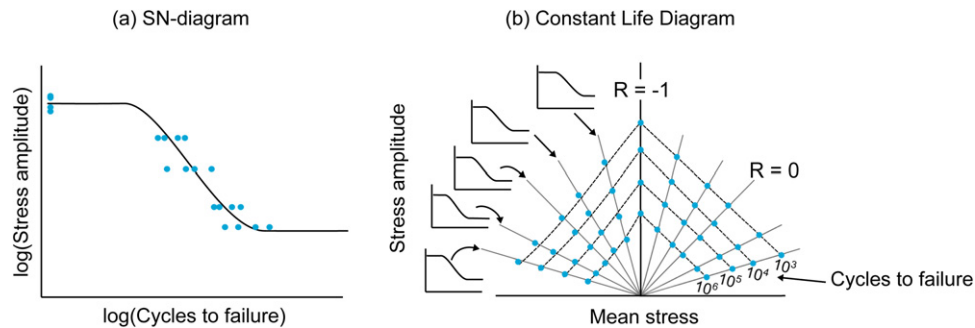


Fig. 9 Example of (a) an SN-diagram and (b) a constant life diagram.

lightly loaded region of the bond line does not contribute much to the static joint strength, including a sufficiently long overlap can be an important design measure to resist creep loading.

Fatigue

Fatigue is the gradual degradation and eventual failure of material due to the application of fluctuating load cycles below the quasi-static strength of the material. Like most other engineering materials, adhesives also suffer from fatigue. Predicting the fatigue behavior of an adhesive joint is therefore crucial to ensuring long term durability of the joint. Various methods have been developed for predicting the fatigue life of a joint, as e.g., reviewed in (Abdel Wahab, 2012; Ashcroft, 2018; Ashcroft and Mubashar, 2021; Vassilopoulos, 2015a). Although modeling techniques are available, they are not yet accurate enough to be used without supporting experiments (Ashcroft, 2018).

The available methods for dealing with fatigue can be roughly classified into three categories (Ashcroft and Mubashar, 2021): total life models, strength and stiffness wear-out approaches, and fracture mechanics approaches. At very low loading frequencies, creep effects may occur during the portion of the load cycle spent at high load, in which case either suitably adjusted data is required, or specific time-dependent methods may be called for (Al-Ghamdi, 2013; Ashcroft, 2018). On the other hand, at high loading frequencies (say > 10 Hz, but this depends on the adhesive), self-heating of the adhesive may occur, which could affect the material properties. This is particularly relevant to take into account for accelerated fatigue testing methods, where one desires to employ high loading frequencies to decrease the test duration. In service, such loading frequencies are typically less common, though they could still occur in specific applications.

Total life models

Total life models are based on experimental data, where cycles with a constant stress amplitude $S_a = 0.5 \cdot (S_{\max} - S_{\min})$ are applied to a specimen until it fails. This is repeated for different values of stress amplitude, and the number of cycles until failure N_f is recorded in each case. This data is then plotted in the form of an SN-diagram, an example of which is shown in Fig. 9(a). Typically a lower asymptote can be seen in the data, implying that below a certain stress amplitude, no fatigue failure will occur. This is known as the fatigue limit. If the stresses in the adhesive bond are kept below the fatigue limit, then no fatigue damage will naturally initiate. However, if damage is somehow created by a different source (e.g., a manufacturing defect, or some in-service event), then loads below the fatigue limit could still cause this damage to grow. Furthermore, as schematically indicated in Fig. 9(a), significant scatter is typically seen in the fatigue lives at any given stress amplitude. Therefore, when relying on SN data, enough data should be collected to allow a proper statistical analysis. Additionally, the use of conservative safety factors on either the load or the design life should be considered.

A tricky question is which stress to use in plotting the SN diagram, given the complex stress distribution in adhesive bonds. Wahab *et al.* (2001) present a comparison of the performance of different stress and strain-based criteria to predict the fatigue limit. The prediction accuracy depended on the environmental conditions, and likely is also geometry dependent. A way to avoid this issue is to plot the graph in terms of the applied force, rather than the stress, as e.g., in Sarfaraz *et al.* (2011), but in that case the results of course only apply to the specific geometry tested.

Apart from the environment, an SN diagram is also specific to only one value of mean stress, which can be alternatively stated as the SN-diagram being dependent on the R -ratio ($R = S_{\min}/S_{\max}$). To take this into account, SN-diagrams can be created for different R -ratios, and then combined into a so-called Constant Life Diagram (CLD), as illustrated schematically in Fig. 9(b). In this diagram one plots the different combinations of mean stress and stress amplitude (or mean force and force amplitude) that result in the same number of cycles to failure (i.e., "constant life"). By interpolating between the experimental data, the life can be predicted for combinations of mean and amplitude stress that were not tested. As reviewed by Vassilopoulos (2015b), many different interpolation models have been developed, including piecewise-linear, linear, and non-linear models. These models have in common that they are all based on empirical fitting of the experimental data, rather than an underlying physical theory of fatigue.

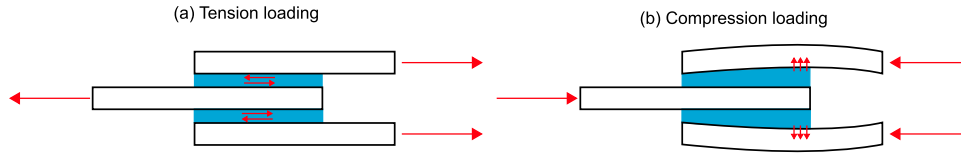


Fig. 10 Schematic illustration of the change in stress distribution in a double lap joint between tensile and compressive axial loading.

Fig. 9(b) illustrates that for an adhesive bond, the CLD is typically not symmetrical. This is because switching from tensile to compressive loading can change the nature of the stresses in the adhesive bond. Consider for example the double lap joint illustrated in **Fig. 10**. If a tensile axial load is applied, the adhesive is mainly subjected to shear stresses. However, if a compressive load is applied and the outer arms are relatively slender, they may start to buckle. In that case the adhesive will be exposed to peel stresses. This will also result in transverse stresses in the inner adherend, which could lead to adherend failure if the adherend is made from a material with low transverse strength, e.g., a fiber reinforced polymer composite. This example should make it clear that different failure modes might be expected if one compares the behavior under tension-tension, tension-compression or compression-compression load cycles. This change of failure modes then translates to quite different fatigue lives for the same absolute values of mean stress and amplitude. A practical example of this can be seen in the investigation of [Sarfaraz et al. \(2011\)](#) who tested double lap joints with glass fiber reinforced polymer adherends. Under tension loading the joint failed through a crack which ran along the bond line, while under compression the joint failed due to a crack which ran along the mid-plane of the inner adherend.

Strength and stiffness wear-out

The total life methods provide the life of the joint, but do not give any information on the development of damage, or the degradation of the joint properties during the life. This has led to the development of phenomenological strength or stiffness wear-out models ([Ashcroft, 2018](#); [Ashcroft and Mubashar, 2021](#)). In these models, the state of the joint is characterized by the residual stiffness or strength, which are measurable properties. The downside of using residual stiffness is that it may not be very sensitive to initial states of damage, whereas the residual strength requires destructive testing to measure ([Ashcroft, 2018](#)). A typical strength wear-out model takes the form ([Ashcroft and Mubashar 2021](#)):

$$S_R(n) = S_u - f(S_u, S_{max}, R)n^\kappa \quad (6)$$

Where $S_R(n)$ is the residual strength after n cycles, S_u is the ultimate tensile strength, S_{max} is the maximum applied stress in the cycle, R is the stress ratio and κ is a strength degradation parameter. The lifetime of the specimen is reached when $S_R(n)$ becomes equal to S_{max} . As a specific model [Ashcroft and Mubashar \(2021\)](#) substitute the failure criterion $S_R(N_f) = S_{max}$ into [eq. 6](#), to give:

$$S_R(n) = S_u - (S_u - S_{max}) \left(\frac{n}{N_f} \right)^\kappa \quad (7)$$

Similarly, one can instead relate the stiffness degradation to a power-law function of the number of cycles ([Yang et al., 1990](#)). Selecting an appropriate failure criterion is not as obvious as for strength wear-out models, [Ashcroft and Mubashar \(2021\)](#) suggest relating the failure stiffness $E(N_f)$ to stress, e.g.:

$$\frac{E(N_f)}{E(0)} = \frac{S_{max}}{S_u} \quad (8)$$

Within finite element analyses, such phenomenological approaches can be incorporated via the concept of damage mechanics. In damage mechanics models the damage is not modeled explicitly. Instead the damage is represented by degradation of specific material properties in a specific area (e.g., certain elements). Essentially, a stiffness or strength wear-out model is used to relate the amount of degradation to the local stress and the number of applied cycles. For a further overview on such approaches, see for example ([Ashcroft et al., 2010](#); [Ashcroft and Mubashar, 2021](#); [Shenoy et al., 2010](#); [Wahab et al., 2001](#)).

Fracture mechanics models

Fracture mechanics models are based on explicit modeling of the growth of cracks in the adhesive. A variety of models have been developed for this purpose, taking into account different factors such as the mode-mixity, temperature, and the R-ratio effect. For a review of these models, see [Pascoe et al. \(2013a\)](#). Given the similarity in damage modes, methods for prediction of delamination growth in composites can also be used to predict the growth of cracks in an adhesive. The basic form of the fracture mechanics models is based on the Paris equation for crack growth in metals ([Paris et al., 1961](#)), restated based on the strain energy release rate:

$$\frac{da}{dN} = Cf(G)^n$$

$$f(G) = G_{max,or}\Delta G_{or}\Delta\sqrt{G} \quad (9)$$

Where da/dN is the crack growth rate and C and n are empirically determined curve fitting parameters, G_{max} represents the SERR at the maximum applied load, $\Delta G = G_{max} - G_{min}$ and $\Delta\sqrt{G} = \sqrt{G_{max}} - \sqrt{G_{min}}$. Which specific formulation to use is still a matter of

debate in the literature. In principle each choice of $f(G)$ can give good predictions, if calibrated with suitable experimental data. Similarly, regardless of which formulation of $f(G)$ is chosen, the coefficient and exponent in Eq. 9 will depend on the R -ratio. This is because a single parameter, whether G_{\max} , ΔG , or $\Delta\sqrt{G}$ is insufficient to uniquely characterize a load cycle, and thus a second parameter (e.g., the R -ratio) is needed (Pascoe *et al.*, 2017). Recently Jones *et al.* (2021) have therefore proposed the use of the equation:

$$\frac{da}{dN} = C\Delta\kappa^n = C \left[\frac{\Delta\sqrt{G} - \Delta\sqrt{G_{thr}}}{\sqrt{1 - \frac{\sqrt{G_{max}}}{A}}} \right]^n \quad (10)$$

Where A is a curve fitting parameter roughly equivalent to the fracture toughness, and the subscript thr refers to the threshold value, below which no crack growth occurs. The advantage of this equation is that various effects, including that of scatter, or of the adhesive thickness (Jones *et al.*, 2021) can be captured within the term $\Delta\kappa$, which therefore becomes a valid similitude parameter. I.e., for two different adhesive bonds, at the same value of $\Delta\kappa$, the same crack growth rate can be observed. Furthermore, note that Eq. 10 contains two different parameters that specify the load cycle, i.e., G_{\max} and $\Delta\sqrt{G}$. Consequently, a given value of $\Delta\kappa$ does not uniquely specify a load cycle, meaning Eq. 10 can capture the R -ratio effect.

Fracture mechanics methods can be incorporated in finite elements via the virtual crack closure technique (Deobald *et al.*, 2017; Pirondi *et al.*, 2014) or cohesive zone models (De Moura and Gonçalves, 2014; Moreira *et al.*, 2020; Pirondi *et al.*, 2016; Pirondi and Moroni, 2019; Rocha *et al.*, 2020). An advantage of the cohesive zone model is that it can include the crack initiation, whereas standard fracture mechanics requires an initial damage to be assumed (Khoramishad *et al.*, 2010).

By explicitly modeling the crack growth, the residual strength and stiffness of the joint after any number of cycles can in principle be calculated, as long as it can be related to the crack length. The fatigue life of the joint has been reached once the crack reaches a critical length, where application of the maximum load in the load cycle causes the strain energy release rate to exceed the fracture toughness of the adhesive, i.e., $G > G_c$. Because fracture mechanics methods rely on modeling the crack explicitly, additional considerations are required when there are multiple cracks, either in the adhesive (Goutianos and Sørensen, 2016; Pascoe *et al.*, 2013b), or in the adherends as well (Adamos and Loutas, 2021).

Variable amplitude fatigue

The methods discussed above are applicable to constant amplitude fatigue. In case of variable load amplitude, further considerations are required. In general, modeling of variable amplitude fatigue behavior is not yet a solved problem, but various approaches can be used to gain some initial estimates of the fatigue behavior.

For total life-models, the Palmgren-Miner rule can be applied, which states that failure occurs when:

$$\sum \frac{n_i}{N_{fi}} = 1 \quad (11)$$

where n_i is the number of applied cycles at the i -th stress level, and N_{fi} is the number of cycles to failure at the i -th applied stress level. The Palmgren-Miner rule is simple to use, but comes with a number of serious limitations. In particular, the rule ignores that stress cycles below the fatigue limit can contribute to the growth of a crack that was initiated due to prior larger amplitude cycles. Furthermore, the rule does not take into account that failure will occur as soon as the residual strength of the sample is reduced to the level of the maximum applied stress in the spectrum. Ashcroft and Mubashar (2021) review a number of possible variations to the Palmgren-Miner rule to compensate for such effects. These include setting the right-hand side of Eq. 11 to a value other than one, or devising non-linear accumulation rules. These may produce good predictions in specific cases, but the general conclusion should be to only apply the Palmgren-Miner rule with caution, and to seek experimental validation of any predictions.

Strength wear-out models that take into account variable amplitude have been proposed by Schaff and Davidson (1997a,b) and Erpolat *et al.* (2004). Erpolat *et al.* showed their model produced more accurate predictions than the Palmgren-Miner rule for the cases they investigated.

With fracture mechanics based methods, variable amplitude can be accounted for if one assumes that linear damage application applies. This assumption essentially states that the crack growth in a specific cycle does not depend on the previously applied load history. The crack growth can then be predicted by a numerical integration of the chosen crack growth law (e.g., Eq. 9), taking into account that in general G is a function of the crack length. Although straightforward to implement, the validity of the linear damage accumulation assumption is questionable and has been shown to underestimate the actual crack growth (Ashcroft and Mubashar, 2021). Therefore, experimental validation of the crack growth predictions remains necessary.

Testing of Adhesive Bonds

Testing of adhesive bonds is important for a variety of reasons, including generation of material data, material screening, quality control, and validation of prediction and analysis models. A wide array of tests have been developed for different purposes, such as testing the bulk adhesive properties, finding joint strengths or fracture toughnesses, or testing the creep or fatigue behavior. Organizations such as ASTM International and the International Organization for Standardization (ISO) have published a range of standards for conducting such tests. A dedicated handbook has been published by da Silva *et al.* (2012) and many handbooks for

adhesive bonding also contain dedicated articles on testing, including e.g., (Adams *et al.*, 1997; Brockmann *et al.*, 2009; da Silva *et al.*, 2018b; Ebnesajjad, 2008). Additionally, Budzik *et al.* (2021) have recently published a review of available test methods, including those applied in specific industrial sectors, such as aerospace, wind energy, civil engineering, and automotive. Budzik *et al.* highlight that many adhesive test standards were originally developed in the aerospace industry, and therefore reflect aerospace structural applications, i.e., thin (1–2 mm) adherends joined by thin (< 1 mm) adhesive layers. These standards do not always well represent applications in other sectors. Consequently, industry still relies a lot on in-house testing procedures, rather than internationally formalized standards.

A variety of methods are available for testing the bulk material properties, the most straightforward of which is tensile testing of dogbone-shaped specimens. For shear properties, commonly used tests are the Iosipescu (V-Notched Beam) test, as standardized in ASTM D5379, and the Arcan (V-Notched plate) test. Both the Iosipescu and Arcan tests involve loading a specimen containing two v-notches. The differences lie in the dimensions of the specimen, and the details of the load introduction into the specimen.

For testing the bond strength, the single lap joint test (see Fig. 1), as covered by ASTM D1002–10 (metal adherends), ASTM D3163 (rigid plastic adherends), ASTM D5868–01 (fiber reinforced plastic adherends) and ISO 4587 (rigid adherends) is very popular. To reduce issues with secondary bending, though at the cost of increased manufacturing effort, one can instead opt for a double lap joint, per ASTM D3528. For a better view of the adhesive shear properties, one can also employ the thick-adherend shear test, per ISO 11003–2 and ASTM D3983. This test is also suitable for fatigue experiments (Budzik *et al.*, 2021). The previously mentioned tests are suitable for rigid adherends. For flexible adherends a peel test (e.g., ASTM D3167, ASTM D1876 or ISO 11339) is more suited.

For fracture mechanics there are few standards available for adhesive bonds. However, within the research community there are a number of test configurations that have become de facto standards, and efforts to develop more formal standards are underway (Brunner *et al.*, 2021). Commonly used geometries include the double cantilever beam (DCB) for mode I testing, the 3 point and 4 point end notched flexure (ENF) and end loaded split (ELS) tests for mode II testing and the mixed mode bending (MMB) test, as the name suggests, for mixed-mode crack growth. For the DCB test ISO 25217 is available for adhesive bonds. For the other configurations, the geometry and general test set-up can be based on available standards for delamination of fiber reinforced polymer composites. For example ASTM D5528 can be used as a basis for DCB tests. For the 3 point ENF there is ASTM D7905. For the ELS test there is a standard under development for adhesives (Brunner *et al.*, 2021) based on ISO 15114 for composites. The MMB test is specified in ASTM D6671.

A detailed discussion of all the available test methods is outside the scope of this article, but some general remarks will be made here. Firstly it is important to realize that unless one is performing a bulk adhesive test, so-called “adhesive” test methods are actually testing a combination of adherends, adhesive, and surface preparation method. The influence of the different components will vary from test to test, but in nearly all tests changing the adherend material or geometry, or changing the surface treatment will affect the outcome of the test, e.g., the failure mode and measured failure load. If this is not correctly taken into account during analysis of the test results, it could give the false impression that generic adhesive material properties are being measured, rather than specimen-specific properties.

As a concrete example, we can look at the single lap joint test, as for example standardized in ASTM D1002 and ISO 4587. This test is very popular because it is relatively cheap and easy to perform. The single lap joint test consists of manufacturing single lap joint specimens, as illustrated in Fig. 1, typically with a width of 25 mm. These specimens are then loaded in tension along the length axis until failure, and the failure load divided by the overlap area (i.e., the average shear stress at failure) is reported. From the discussion on stress analysis (Fig. 3) it should be clear that this average shear stress is not a good representation of the stress distribution in the adhesive. Therefore the average shear stress cannot be used to predict the failure of the same adhesive for different geometries, including even different overlap lengths. Nevertheless, the results can easily be compared to those from other single lap joint tests conducted according to the same standard. This makes the test very suitable for purposes such as material screening or quality control. Although this test is thought of an adhesive test, the properties of the adherends, especially their thickness and stiffness, will influence the measured failure load, as can be seen in e.g., Eqs. 2 and 3. The adherend properties can also affect the failure mode. For example, failure could occur through yielding of the adherends if they are too thin or weak (da Silva *et al.*, 2012). Similarly a difference in surface preparation could change the failure mode from cohesive to adhesive.

In short, the issues discussed above illustrate the importance of carefully selecting the right test to provide the needed data for a given joint. Particular care is needed if a test is being conducted in order to qualify a design or analyze an in-service failure. If a test coupon is being used, rather than a full-scale structure, the geometry of the bond area, particularly the number of overlaps, the overlap length, and the presence of stress raisers, should still be matched as closely as possible. Furthermore the adherend stiffnesses and thicknesses should match, as well as the used manufacturing process (especially the surface treatment). The test temperature and humidity should match the operational environment, and pre-conditioning of the specimens to induce moisture absorption should be considered. Finally, it is important to ensure that the failure mode seen during the test is the same as the failure mode that is seen or expected in service. If the failure mode that occurs during the test does not match the one seen in service, the test will have very little predictive power.

Summary and Conclusion

This article has covered the failure analysis of adhesive bonds. It has illustrated that the stress distribution within an adhesive bond is complex, and that different methods exist for analyzing it. These range from relatively simple analytical methods of limited

accuracy to more complex and accurate methods, with finite element methods being required for complex geometries. The importance of conducting a non-linear analysis in the case of ductile adhesives was highlighted. An overview was given of different failure criteria that can be used to predict the bond strength, where it must be noted that a failure criterion will only be reliable if the failure mode does not change.

The strength of an adhesive bond depends not just on the geometry and materials used, but also on the suitability and quality of the manufacturing process, and on environmental effects such as temperature and moisture. To ensure long term durability and structural integrity, the possibility of creep and fatigue should be investigated, and available methods for this were reviewed.

Given the uncertainties in available models, experimental testing is indispensable to validate analyses, as well as to generate the necessary input data. Many test methods are available, and selecting the right method requires careful consideration of the purpose of the test and of possible influencing factors.

Highlights

- The stress distribution in an adhesive bond is complex. Relying on the average shear stress for failure analysis is misleading
- An overview is given of different stress analysis methods and failure criteria.
- The influence of manufacturing and of the operating environment is discussed.
- Different methods for analyzing creep and fatigue loading are presented.

References

- Abdel Wahab, M.M., 2012. Fatigue in adhesively bonded joints: A review. *ISRN Mater. Sci.* 2012, 1–25. <https://doi.org/10.5402/2012/746308>.
- Adamos, L., Loutas, T., 2021. Challenges in the fatigue crack growth characterization of metal/composite joints: A compliance-based investigation of a Ti/CFRP joint. *Int. J. Fatigue* 148, 106233. <https://doi.org/10.1016/j.ijfatigue.2021.106233>.
- Adams, R.D., 1989. Strength predictions for lap joints, especially with composite adherends. A review. *J. Adhes.* 30, 219–242. <https://doi.org/10.1080/00218468908048207>.
- Adams, R.D., Peppiatt, N.A., 1973. Effect of poisson's ratio strains in adherends on stresses of an idealized lap joint. *J. Strain Anal. Eng. Des.* 8, 134–139. <https://doi.org/10.1243/03093247V082134>.
- Adams, R.D., Peppiatt, N.A., 1974. Stress analysis of adhesively-bonded lap joints. *J. Strain Anal.* 9, 185–196. <https://doi.org/10.1243/03093247V093185>.
- Adams, R.D., Mallick, V., 1992. A method for the stress analysis of lap joints. *J. Adhes.* 38, 199–217. <https://doi.org/10.1080/00218469208030455>.
- Adams, R.D., Comyn, J., Wake, W.C., 1997. *Structural Adhesive Joints in Engineering*, second ed. London: Chapman & Hall,.
- Akhavan-Safar, A., Ayatollahi, M.R., da Silva, L.F.M., 2017. Strength prediction of adhesively bonded single lap joints with different bondline thicknesses: A critical longitudinal strain approach. *Int. J. Solids Struct.* 109, 189–198. <https://doi.org/10.1016/j.ijsolstr.2017.01.022>.
- Akhavan-Safar, A., Marques, E.A.S., Carbas, R.J.C., da Silva, L.F.M., 2021. Stress analysis of adhesive joints. In: Adams, R.D. (Ed.), *Adhesive Bonding - Science, Technology and Applications*. Duxford: Woodhead Publishing, pp. 159–192. <https://doi.org/10.1016/b978-0-12-819954-1.00020-4>.
- Al-Ghamdi, A.H., 2013. *Fatigue and Creep of Adhesively Bonded Joints* (PhD Thesis). Loughborough University.
- Ambrose, S.H., 1998. Chronology of the later stone age and food production in East Africa. *J. Archaeol. Sci.* 25, 377–392. <https://doi.org/10.1006/jasc.1997.0277>.
- Arouche, M.M., Teixeira de Freitas, S., de Barros, S., 2021. Evaluation of the strain-based partitioning method for mixed-mode I+II fracture of bi-material cracks. *J. Adhes.* 00, 1–29. <https://doi.org/10.1080/00218464.2021.1981297>.
- Ashcroft, I.A., 2018. Fatigue load conditions. In: da Silva, L.F.M., Öchsner, A., Adams, R.D. (Eds.), *Handbook of Adhesion Technology: Second Edition*. Cham: Springer, pp. 941–975.
- Ashcroft, I.A., Mubashar, A., 2018. Numerical approach: Finite element analysis. In: da Silva, L.F.M., Öchsner, A., Adams, R.D. (Eds.), *Handbook of Adhesion Technology: Second Edition*. Cham: Springer, pp. 701–740.
- Ashcroft, I.A., Mubashar, A., 2021. Fatigue. In: Adams, R.D. (Ed.), *Adhesive Bonding - Science, Technology and Applications*. Duxford: Woodhead Publishing, pp. 317–361. <https://doi.org/10.1016/B978-0-12-819954-1.00006-X>.
- Ashcroft, I.A., Digby, R.P., Shaw, S.J., 2001. A comparison of laboratory-conditioned and naturally-weathered bonded joints. *J. Adhes.* 75, 175–201. <https://doi.org/10.1080/00218460108029600>.
- Ashcroft, I.A., Comyn, J., Mubashar, A., 2018. Effect of water and mechanical stress on durability. In: da Silva, L.F.M., Öchsner, A., Adams, R.D. (Eds.), *Handbook of Adhesion Technology: Second Edition*. Cham: Springer, pp. 879–914.
- Ashcroft, I.A., Shenoy, V., Critchlow, G.W., Crocombe, A.D., 2010. A comparison of the prediction of fatigue damage and crack growth in adhesively bonded joints using fracture mechanics and damage mechanics progressive damage methods. *J. Adhes.* 86, 1203–1230. <https://doi.org/10.1080/00218464.2010.529383>.
- Ayatollahi, M.R., Akhavan-Safar, A., 2015. Failure load prediction of single lap adhesive joints based on a new linear elastic criterion. *Theor. Appl. Fract. Mech.* 80, 210–217. <https://doi.org/10.1016/j.tafmec.2015.07.013>.
- Azari, S., Papini, M., Spelt, J.K., 2011. Effect of adhesive thickness on fatigue and fracture of toughened epoxy joints - Part I: Experiments. *Eng. Fract. Mech.* 78, 153–162. <https://doi.org/10.1016/j.engfracmech.2010.06.025>.
- Bigwood, D.A., Crocombe, A.D., 1989. Elastic analysis and engineering design formulae for bonded joints. *Int. J.* 9, 229–242. [https://doi.org/10.1016/0143-7496\(89\)90066-3](https://doi.org/10.1016/0143-7496(89)90066-3).
- Bigwood, D.A., Crocombe, A.D., 1990. Non-linear adhesive bonded joint design analyses. *Int. J. Adhes. Adhes.* 10, 9. [https://doi.org/10.1016/0143-7496\(90\)90010-u](https://doi.org/10.1016/0143-7496(90)90010-u).
- Bisagni, C., Furlari, D., Pacchione, M., 2018. Experimental investigation of reinforced bonded joints for composite laminates. *J. Compos. Mater.* 52, 431–447.
- Borges, C.S.P., Marques, E.A.S., Carbas, R.J.C., et al., 2021. Review on the effect of moisture and contamination on the interfacial properties of adhesive joints. *Proc. Inst. Mech. Eng. Part C J. Mech. Eng. Sci.* 235, 527–549. <https://doi.org/10.1177/0954406220944208>.
- Brockmann, W., Geiß, P.L., Klöng, J., Schröder, B., Mikhail, B., 2009. *Adhesive Bonding - Materials Applications & Technology*. Weinheim: Wiley-VCH.
- Brunner, A.J., Warnet, L., Blackman, B.R.K., 2021. 35 years of standardization and research on fracture of polymers, polymer composites and adhesives in ESIS TC4: Past achievements and future directions. *Procedia Struct. Integr.* 33, 443–455. <https://doi.org/10.1016/j.prostr.2021.10.051>.
- Budhe, S., Banea, M.D., de Barros, S., da Silva, L.F.M., 2017. An updated review of adhesively bonded joints in composite materials. *Int. J. Adhes. Adhes.* 72, 30–42. <https://doi.org/10.1016/j.ijadhadh.2016.10.010>.
- Budzik, M.K., Wolfahrt, M., Reis, P., et al., 2021. Testing mechanical performance of adhesively bonded composite joints in engineering applications: An overview. *J. Adhes.* 00, 1–77. <https://doi.org/10.1080/00218464.2021.1953479>.
- Chen, Y., Smith, L.V., 2020. A nonlinear viscoelastic-viscoplastic model for adhesives. *Mech. Time-Depend. Mater.* 565–579. <https://doi.org/10.1007/s11043-020-09460-2>.

- Cheng, S., Chen, D., Shi, Y., 1991. Analysis of adhesive-bonded joints with nonidentical adherends. *J. Eng. Mech.* 117, 605–623.
- Chiu, W.K., Rees, D., Chalkey, P., Jones, R., 1994. Designing for damage-tolerant composite repairs. *Compos. Struct.* 28, 19–37. [https://doi.org/10.1016/0263-8223\(94\)90003-5](https://doi.org/10.1016/0263-8223(94)90003-5).
- Chowdhury, N.M., Wang, J., Chiu, W.K., Chang, P., 2016. Static and fatigue testing bolted, bonded and hybrid step lap joints of thick carbon fibre/epoxy laminates used on aircraft structures. *Compos. Struct.* 142, 96–106. <https://doi.org/10.1016/j.compstruct.2016.01.078>.
- Comyn, J., 2021. *Environmental ((durability)) Effects*, second ed. Duxford: Adhesive Bonding. Woodhead Publishing, <https://doi.org/10.1016/b978-0-12-819954-1.00009-5>.
- Critchlow, G., 2018. General introduction to surface treatments. In: da Silva, L.F.M., Öchsner, A., Adams, R.D. (Eds.), *Handbook of Adhesion Technology: Second Edition*. Cham: Springer, pp. 131–162.
- Croccombe, A.D., 1989. Global yielding as a failure criterion for bonded joints. *Int. J. Adhes. Adhes.* 9, 145–153. [https://doi.org/10.1016/0143-7496\(89\)90110-3](https://doi.org/10.1016/0143-7496(89)90110-3).
- Croccombe, A.D., 2008. Incorporating environmental degradation in closed form adhesive joint stress analyses. *J. Adhes.* 84, 212–230. <https://doi.org/10.1080/00218460801954268>.
- Croccombe, A.D., Adams, R.D., 1981. Influence of the spew fillet and other parameters on the stress distribution in the single lap joint. *J. Adhes.* 13, 141–155. <https://doi.org/10.1080/00218468108073182>.
- Croccombe, A.D., Ashcroft, I.A., 2008. Simple lap joint geometry. In: da Silva, L.F.M., Öchsner, A. (Eds.), *Modeling of Adhesively Bonded Joints*. Verlag, Berlin: Springer, pp. 3–23. https://doi.org/10.1007/978-3-540-79056-3_1.
- De Moura, M.F.S.F., Gonçalves, J.P.M., 2014. Cohesive zone model for high-cycle fatigue of adhesively bonded joints under mode I loading. *Int. J. Solids Struct.* 51, 1123–1131. <https://doi.org/10.1016/j.ijsolstr.2013.12.009>.
- De Sousa, C.C.R.G., Campilho, R., Marques, E.A.S., Costa, M., Da Silva, L.F.M., 2017. Overview of different strength prediction techniques for single-lap bonded joints. *Proc. Inst. Mech. Eng. Part L J. Mater. Des. Appl.* 231, 210–223. <https://doi.org/10.1177/1464420716675746>.
- Deobald, L.R., Mabson, G.E., Engelstad, S., *et al.*, 2017. Guidelines for VCCT-based Interlaminar Fatigue and Progressive Failure Finite Element Analysis, NASA/TM-2017-219663.
- Dillard, D.A., 2021. *Applying Fracture Mechanics to Adhesive Bonds*, second ed. Adhesive Bonding. Elsevier Ltd., <https://doi.org/10.1016/b978-0-12-819954-1.00014-9>.
- Doru, M.O., Özel, A., Akpınar, S., Aydın, M.D., 2014. Effect of the spew fillet on adhesively bonded single-lap joint subjected to tensile loading: Experimental and 3-D non-linear stress analysis. *J. Adhes.* 90, 195–209. <https://doi.org/10.1080/00218464.2013.777900>.
- Durodola, J.F., 2017. Functionally graded adhesive joints – A review and prospects. *Int. J. Adhes. Adhes.* 76, 83–89. <https://doi.org/10.1016/j.ijadhadh.2017.02.008>.
- Ebnesajjad, S., 2008. *Adhesives Technology Handbook*, second ed. Norwich, NY: William Andrews.
- Erpolat, S., Ashcroft, I.A., Croccombe, A.D., Abdel-Wahab, M.M., 2004. A study of adhesively bonded joints subjected to constant and variable amplitude fatigue. *Int. J. Fatigue* 26, 1189–1196. <https://doi.org/10.1016/j.ijfatigue.2004.03.011>.
- Federal Aviation Administration, 2010. Advisory Circular AC20-107B: Composite Aircraft Structure.
- Geiss, P.L., Vogt, D., 2005. Assessment and prediction of long-term mechanical properties of adhesives with high plasticity. *J. Adhes. Sci. Technol.* 19, 1291–1303. <https://doi.org/10.1163/156856105774784385>.
- Geiß, P.L., Schumann, M., 2018. Creep load conditions. In: da Silva, L.F.M., Öchsner, A., Adams, R.D. (Eds.), *Handbook of Adhesion Technology: Second Edition*. Cham: Springer, pp. 975–1008.
- Gleich, D.M., Van Tooren, M.J.L., Beukers, A., 2001. Analysis and evaluation of bondline thickness effects on failure load in adhesively bonded structures. *J. Adhes. Sci. Technol.* 15, 1091–1101. <https://doi.org/10.1163/156856101317035503>.
- Gleich, D., 2002. *Stress Analysis of Structural Bonded Joints* (PhD Thesis). Delft University of Technology.
- Goh, J.Y., Georgiadis, S., Orifici, A.C., Wang, C.H., 2013. Effects of bondline flaws on the damage tolerance of composite scarf joints. *Compos. Part A Appl. Sci. Manuf.* 55, 110–119. <https://doi.org/10.1016/j.compositesa.2013.07.017>.
- Goland, M., Reissner, E., 1944. The stresses in cemented joints. *J. Appl. Mech.* 11, A17–A27. <https://doi.org/10.1115/1.4009336>.
- Goutianos, S., Sørensen, B.F., 2016. Fracture resistance enhancement of layered structures by multiple cracks. *Eng. Fract. Mech.* 151, 92–108. <https://doi.org/10.1016/j.engfracmech.2015.10.036>.
- Hart-Smith, L.J., 1981. Further developments in the design and analysis of adhesive bonded structural joints. *ASTM Spec. Tech. Publ.* 3–31. <https://doi.org/10.1520/stp33472s>.
- Hart-Smith, L.J., 1973a. Adhesive-Bonded Single-Lap Joints (No. NASA CR-112236). Hampton, VA.
- Hart-Smith, L.J., 1973b. Adhesive Bonded Double-Lap Joints (No. NASA CR-112235). Hampton, VA.
- Hisada, S., Minakuchi, S., Takeda, N., 2020. Damage tolerance improvement of composite T-joint under pull-up conditions using an interlocking-fiber-based crack arrester. *Compos. Struct.* 253, 112792. <https://doi.org/10.1016/j.compstruct.2020.112792>.
- Jiang, Z., Fang, Z., Yan, L., Wan, S., Fang, Y., 2021. Mixed-mode I/II fracture criteria for adhesively-bonded pultruded GFRP/steel joint. *Compos. Struct.* 255, 113012. <https://doi.org/10.1016/j.compstruct.2020.113012>.
- Jones, R., Chiu, W.K., Paul, J., 1993. Designing for damage tolerant bonded joints. *Compos. Struct.* 25, 201–207. [https://doi.org/10.1016/0263-8223\(93\)90166-N](https://doi.org/10.1016/0263-8223(93)90166-N).
- Jones, R., Kinloch, A.J., Michopoulos, J., Iliopoulos, A.P., 2021. Crack growth in adhesives: Similarity and the Hartman-Schijve equation. *Compos. Struct.* 273, 114260. <https://doi.org/10.1016/j.compstruct.2021.114260>.
- Jones, R., Peng, D., Michopoulos, J.G., Phan, N., Berto, F., 2018. On the analysis of bonded step lap joints. *Theor. Appl. Fract. Mech.* 97, 457–466. <https://doi.org/10.1016/j.tafmec.2017.09.001>.
- Kasper, Y., Albiez, M., Ummerhofer, T., *et al.*, 2021. Application of toughened epoxy-adhesives for strengthening of fatigue-damaged steel structures. *Constr. Build. Mater.* 275, 121579. <https://doi.org/10.1016/j.conbuildmat.2020.121579>.
- Kemal Apalak, M., Davies, R., 1994. Analysis and design of adhesively bonded corner joints: Fillet effect. *Int. J. Adhes. Adhes.* 14, 163–174. [https://doi.org/10.1016/0143-7496\(94\)90026-4](https://doi.org/10.1016/0143-7496(94)90026-4).
- Khabazaghdam, A., Behjat, B., Yazdani, M., *et al.*, 2021. Creep behaviour of a graphene-reinforced epoxy adhesively bonded joint: experimental and numerical investigation. *J. Adhes.* 97, 1189–1210. <https://doi.org/10.1080/00218464.2020.1742114>.
- Khoramishad, H., Croccombe, A.D., Katnam, K.B., Ashcroft, I.A., 2010. Predicting fatigue damage in adhesively bonded joints using a cohesive zone model. *Int. J. Fatigue* 32, 1146–1158. <https://doi.org/10.1016/j.ijfatigue.2009.12.013>.
- Kinloch, A.J., Shaw, S.J., 1981. The fracture resistance of a toughened epoxy adhesive. *J. Adhes.* 12, 59–77. <https://doi.org/10.1080/00218468108071189>.
- Klein, B., 1997. *Leichtbau-Konstruktion: Berechnungsgrundlagen und Gestaltung*, third ed. Braunschweig: Vieweg.
- Kruse, T., 2013. Bonding of CFRP primary aerospace structures: Overview on the technology status in the context of the certification boundary conditions addressing needs for development. In: *Proceedings of the 19th International Conference on Composite Materials*. Montreal, p. KRU80405.
- Kruse, T., Koerwien, T., Geistbeck, T.M. M., 2018. Certification by means of Disbond Arrest Features and Results (No. STO-MP-AVT-266).
- Kupski, J., Teixeira de Freitas, S., 2021. Design of adhesively bonded lap joints with laminated CFRP adherends: Review, challenges and new opportunities for aerospace structures. *Compos. Struct.* 268, 113923. <https://doi.org/10.1016/j.compstruct.2021.113923>.
- Kupski, J., Teixeira de Freitas, S., Zarouchas, D., Camanho, P.P., Benedictus, R., 2019. Composite layup effect on the failure mechanism of single lap bonded joints. *Compos. Struct.* 217, 14–26. <https://doi.org/10.1016/j.compstruct.2019.02.093>.
- Leguillon, D., 2002. Strength or toughness? A criterion for crack onset at a notch. *Eur. J. Mech. A/Solids* 21, 61–72. [https://doi.org/10.1016/S0997-7538\(01\)01184-6](https://doi.org/10.1016/S0997-7538(01)01184-6).
- Leguillon, D., Laurencin, J., Dupeux, M., 2003. Failure initiation in an epoxy joint between two steel plates. *Eur. J. Mech. A/Solids* 22, 509–524. [https://doi.org/10.1016/S0997-7538\(03\)00066-4](https://doi.org/10.1016/S0997-7538(03)00066-4).
- Mallik, P.K., 2018. *Processing of Polymer Matrix Composites*. Boca Raton: Taylor & Francis.
- Marques, A.C., Mocanu, A., Tomić, N.Z., *et al.*, 2020. Review on adhesives and surface treatments for structural applications: Recent developments on sustainability and implementation for metal and composite substrates. *Materials* 13, 1–43. <https://doi.org/10.3390/ma13245590>.

- Marques, E.A.S., Carbas, R.J.C., Silva, F., *et al.*, 2017. Use of master curves based on time-temperature superposition to predict creep failure of aluminium-glass adhesive joints. *Int. J. Adhes. Adhes.* 74, 144–154. <https://doi.org/10.1016/j.ijadhadh.2016.12.007>.
- Matlinina, J.P., Lung, C.Y.K., Tsoi, J.K.H., 2018. Silane adhesion mechanism in dental applications and surface treatments: A review. *Dent. Mater.* 34, 13–28. <https://doi.org/10.1142/7114>.
- Mazza, P.P.A., Martini, F., Sala, B., *et al.*, 2006. A new Palaeolithic discovery: Tar-hafted stone tools in a European Mid-Pleistocene bone-bearing bed. *J. Archaeol. Sci.* 33, 1310–1318. <https://doi.org/10.1016/j.jas.2006.01.006>.
- Minakuchi, S., 2015. Fiber-reinforcement-based crack arrester for composite bonded joints. In: *Proceedings of the 20th International Conference on Composite Materials*. Paper 2118–4.
- Moreira, R.D.F., de Moura, M.F.S.F., Silva, F.G.A., Ramirez, F.M.G., Silva, F.D.R., 2020. Numerical comparison of several composite bonded repairs under fatigue loading. *Compos. Struct.* 243, 112250. <https://doi.org/10.1016/j.compstruct.2020.112250>.
- Mueller, E.M., Starnes, S., Strickland, N., Kenny, P., Williams, C., 2016. The detection, inspection, and failure analysis of a composite wing skin defect on a tactical aircraft. *Compos. Struct.* 145, 186–193. <https://doi.org/10.1016/j.compstruct.2016.02.046>.
- Ojalvo, I.U., Eidinoff, H.L., 1978. Bond thickness effects upon stresses in single-lap adhesive joints. *AIAA J.* 16, 204–211.
- Pardoen, T., Ferracin, T., Landis, C.M., Delannay, F., 2005. Constraint effects in adhesive joint fracture. *J. Mech. Phys. Solids* 53, 1951–1983. <https://doi.org/10.1016/j.jmps.2005.04.009>.
- Paris, P.C., Gomez, M.P., Anderson, W.E., 1961. A rational analytic theory of fatigue. *Trend Eng.* 13, 9–14.
- Park, S.Y., Choi, W.J., Choi, H.S., 2018. A review of the recent developments in surface treatment techniques for bonded repair of aluminum airframe structures. *Int. J. Adhes. Adhes.* 80, 16–29. <https://doi.org/10.1016/j.ijadhadh.2017.09.010>.
- Pascoe, J.A., Alderliesten, R.C., Benedictus, R., 2013a. Methods for the prediction of fatigue delamination growth in composites and adhesive bonds - A critical review. *Eng. Fract. Mech.* 112–113, 72–96. <https://doi.org/10.1016/j.engfracmech.2013.10.003>.
- Pascoe, J.A., Rans, C.D., Benedictus, R., 2013b. Characterizing fatigue delamination growth behaviour using specimens with multiple delaminations: The effect of unequal delamination lengths. *Eng. Fract. Mech.* 109, 150–160. <https://doi.org/10.1016/j.engfracmech.2013.05.015>.
- Pascoe, J.A., Alderliesten, R.C., Benedictus, R., 2017. On the physical interpretation of the R-ratio effect and the LFM parameters used for fatigue crack growth in adhesive bonds. *Int. J. Fatigue* 97, 162–176. <https://doi.org/10.1016/j.ijfatigue.2016.12.033>.
- Pascoe, J.A., Zarouchas, D.S., Alderliesten, R.C., Benedictus, R., 2018. Using acoustic emission to understand fatigue crack growth within a single load cycle. *Eng. Fract. Mech.* 194, 281–300. <https://doi.org/10.1016/j.engfracmech.2018.03.012>.
- Pascoe, J.A., Zavatta, N., Troiani, E., Alderliesten, R.C., 2020. The effect of bond-line thickness on fatigue crack growth rate in adhesively bonded joints. *Eng. Fract. Mech.* 229, 106959. <https://doi.org/10.1016/j.engfracmech.2020.106959>.
- Pethrick, R.A., 2015. Design and ageing of adhesives for structural adhesive bonding-A review. *Proc. Inst. Mech. Eng. Part L J. Mater. Des. Appl.* 229, 349–379. <https://doi.org/10.1177/1464420714522981>.
- Pirondi, A., Moroni, F., 2019. Improvement of a cohesive zone model for fatigue delamination rate simulation. *Materials* 12, 1–17. <https://doi.org/10.3390/ma12010181>.
- Pirondi, A., Giuliese, G., Moroni, F., 2016. Fatigue debonding three-dimensional simulation with cohesive zone. *J. Adhes.* 92, 553–571. <https://doi.org/10.1080/00218464.2015.1127764>.
- Pirondi, A., Giuliese, G., Moroni, F., Bernasconi, A., Jamil, A., 2014. Comparative study of cohesive zone and virtual crack closure techniques for three-dimensional fatigue debonding. *J. Adhes.* 90, 457–481. <https://doi.org/10.1080/00218464.2013.859616>.
- Plusinis, D., Spelt, J.K., 1995. Designing for time-dependent crack growth in adhesive joints. *Int. J. Adhes. Adhes.* 15, 143–154. [https://doi.org/10.1016/0143-7496\(95\)91625-G](https://doi.org/10.1016/0143-7496(95)91625-G).
- Potter, D.L., 1979. Primary Adhesively Bonded Structure Technology (PABST) Design Handbook for Adhesive Bonding (No. AFFDL-TR-79-3129).
- Poulis, J.A., Seymour, K., Mosleh, Y., 2020. The influence of loading, temperature and relative humidity on adhesives for canvas lining. *IOP Conf. Ser. Mater. Sci. Eng.* 949.
- Ramalho, L.D.C., Campilho, R.D.S.G., Belinha, J., da Silva, L.F.M., 2020. Static strength prediction of adhesive joints: A review. *Int. J. Adhes. Adhes.* 96, 102451. <https://doi.org/10.1016/j.ijadhadh.2019.102451>.
- Rocha, A.V.M., Akhavan-Safar, A., Carbas, R., *et al.*, 2020. Numerical analysis of mixed-mode fatigue crack growth of adhesive joints using CZM. *Theor. Appl. Fract. Mech.* 106, 102493. <https://doi.org/10.1016/j.tafmec.2020.102493>.
- Sadeghi, M.Z., Zimmermann, J., Gabener, A., Schroeder, K.U., 2018. The applicability of J-integral approach in the determination of mixed-mode fracture energy in a ductile adhesive. *Int. J. Adhes. Adhes.* 83, 2–8. <https://doi.org/10.1016/j.ijadhadh.2018.02.027>.
- Sancaktar, E., 2018. Classification of adhesive and sealant materials. In: da Silva, L.F.M., Öchsner, A., Adams, R.D. (Eds.), *Handbook of Adhesion Technology: Second Edition*. Cham: Springer, pp. 283–318.
- Sarfraz, R., Vassilopoulos, A.P., Keller, T., 2011. Experimental investigation of the fatigue behavior of adhesively-bonded pultruded GFRP joints under different load ratios. *Int. J. Fatigue* 33, 1451–1460. <https://doi.org/10.1016/j.ijfatigue.2011.05.012>.
- Schaff, J.R., Davidson, B.D., 1997a. Life prediction methodology for composite structures. Part II - spectrum fatigue. *J. Compos. Mater.* 31, 158–181.
- Schaff, J.R., Davidson, B.D., 1997b. Life prediction methodology for composite structures. Part I - constant amplitude and two-stress level fatigue. *J. Compos. Mater.* 31, 128–157.
- Seneviratne, W., Tomblin, J., Kittur, M., 2015. Durability and residual strength of adhesively-bonded composite joints: The case of F/A-18 A-D wing root stepped-lap joint. In: Vassilopoulos, A.P. (Ed.), *Fatigue and Fracture of Adhesively-Bonded Composite Joints*. Cambridge: Elsevier Ltd, pp. 289–320. <https://doi.org/10.1016/B978-0-85709-806-1.00010-0>.
- Shang, X., Marques, E.A.S., Machado, J.J.M., *et al.*, 2019. Review on techniques to improve the strength of adhesive joints with composite adherends. *Compos. Part B Eng.* 177, 107363. <https://doi.org/10.1016/j.compositesb.2019.107363>.
- Shenoy, V., Ashcroft, I.A., Critchlow, G.W., Crocombe, A.D., 2010. Fracture mechanics and damage mechanics based fatigue lifetime prediction of adhesively bonded joints subjected to variable amplitude fatigue. *Eng. Fract. Mech.* 77, 1073–1090. <https://doi.org/10.1016/j.engfracmech.2010.03.008>.
- da Silva, L.F.M., Lopes, M.J.C.Q., 2009. Joint strength optimization by the mixed-adhesive technique. *Int. J. Adhes. Adhes.* 29, 509–514. <https://doi.org/10.1016/j.ijadhadh.2008.09.009>.
- da Silva, L.F.M., Campilho, R.D.S.G., 2015. Design of adhesively-bonded composite joints. In *Fatigue and Fracture of Adhesively-Bonded Composite Joints*. Elsevier Ltd. <https://doi.org/10.1016/B978-0-85709-806-1.00002-1>.
- da Silva, L.F.M., Marques, E.A.S., Campilho, R.D.S.G., 2018a. Design rules and methods to improve joint strength. In: da Silva, L.F.M., Öchsner, A., Adams, R.D. (Eds.), *Handbook of Adhesion Technology: Second Edition*. Cham: Springer, pp. 773–810.
- da Silva, L.F.M., Öchsner, A., Adams, R.D., 2018b. *Handbook of Adhesion Technology*, second ed. Cham: Springer.
- da Silva, L.F.M., das Neves, P.J.C., Adams, R.D., Spelt, J.K., 2009a. Analytical models of adhesively bonded joints-Part I: Literature survey. *Int. J. Adhes. Adhes.* 29, 319–330. <https://doi.org/10.1016/j.ijadhadh.2008.06.005>.
- da Silva, L.F.M., Dillard, D.A., Blackman, B.R.K., Adams, R.D., 2012. *Testing Adhesive Joints*. Weinheim: Wiley-VCH.
- da Silva, L.F.M., Rodrigues, T.N.S.S., Figueiredo, M.A.V., de Moura, M.F.S.F., Chousal, J.A.G., 2006. Effect of adhesive type and thickness on the lap shear strength. *J. Adhes.* 82, 1091–1115. <https://doi.org/10.1080/00218460600948511>.
- da Silva, L.F.M., das Neves, P.J.C., Adams, R.D., Wang, A., Spelt, J.K., 2009b. Analytical models of adhesively bonded joints-Part II: Comparative study. *Int. J. Adhes. Adhes.* 29, 331–341. <https://doi.org/10.1016/j.ijadhadh.2008.06.007>.
- Stapleton, S.E., Waas, A.M., Arnold, S.M., 2012. Functionally graded adhesives for composite joints. *Int. J. Adhes. Adhes.* 35, 36–49. <https://doi.org/10.1016/j.ijadhadh.2011.11.010>.
- Steinmetz, J., Löbel, T., Völkerink, O., *et al.*, 2021. The working principles of a multifunctional bondline with disbond stopping and health monitoring features for composite structures. *J. Compos. Sci.* 5, 1–17. <https://doi.org/10.3390/cs5020051>.
- Taylor, D., 2008. The theory of critical distances. *Eng. Fract. Mech.* 75, 1696–1705. <https://doi.org/10.1016/j.engfracmech.2007.04.007>.

- Tong, L., Luo, Q., 2018. Analytical approach. In: da Silva, L.F., Öchsner, A., Adams, R.D. (Eds.), *Handbook of Adhesion Technology: Second Edition*. Cham: Springer, pp. 665–700.
- Tserpes, K., Barroso-Caro, A., Carraro, P.A., *et al.*, 2021. A review on failure theories and simulation models for adhesive joints. *J. Adhes.* 00, 1–61. <https://doi.org/10.1080/00218464.2021.1941903>.
- Usman, M., Pascoe, J.A., Alderliesten, R.C., Benedictus, R., 2018. The effect of temperature on fatigue crack growth in FM94 epoxy adhesive bonds investigated by means of energy dissipation. *Eng. Fract. Mech.* 189, 98–109. <https://doi.org/10.1016/j.engfracmech.2017.10.007>.
- Vassilopoulos, A.P., 2015a. *Fatigue and Fracture of Adhesively-Bonded Composite Joints*. Cambridge: Woodhead Publishing.
- Vassilopoulos, A.P., 2015b. Predicting the fatigue life of adhesively-bonded structural composite joints. In *Fatigue and Fracture of Adhesively-Bonded Composite Joints*. Elsevier Ltd. <https://doi.org/10.1016/B978-0-85709-806-1.00016-1>.
- Volkersen, O., 1938. Die Niekraftverteilung in Zugbeanspruchten mit Konstanten Laschenquerschnitten. *Luftfahrtforschung* 15, 41–47.
- Wadley, L., Hodgskiss, T., Grant, M., 2009. Implications for complex cognition from the hafting of tools with compound adhesives in the Middle Stone Age, South Africa. *Proc. Natl. Acad. Sci. USA* 106, 9590–9594. <https://doi.org/10.1073/pnas.0900957106>.
- Wahab, M.M.A., Ashcroft, I.A., Crocombe, A.D., Hughes, D.J., Shaw, S.J., 2001. Effect of environment on the fatigue of bonded composite joints. Part 2: Fatigue threshold prediction. *Compos. Part A Appl. Sci. Manuf.* 32, 59–69. [https://doi.org/10.1016/S1359-835X\(00\)00132-9](https://doi.org/10.1016/S1359-835X(00)00132-9).
- Wang, W., De Freitas, S.T., Poulis, J.A., Zarouchas, D., 2021. A review of experimental and theoretical fracture characterization of bi-material bonded joints. *Compos. Part B Eng.* 206, 108537. <https://doi.org/10.1016/j.compositesb.2020.108537>.
- Williams, J.G., 1988. On the calculation of energy release rates for cracked laminates. *Int. J. Fract.* 36, 101–119. <https://doi.org/10.1007/s10704-006-0044-0>.
- Wu, E.M., Reuter Jr. R.C., 1965. *Crack Extension in Fiberglass Reinforced Plastics*, Illinois University at Urbana Dept. of Theoretical and Applied Mechanics, Report No. 275.
- Yan, C., Mai, Y.W., Ye, L., 2001. Effect of bond thickness on fracture behaviour in adhesive joints. *J. Adhes.* 75, 27–44. <https://doi.org/10.1080/00218460108029592>.
- Yang, J.N., Jones, D.L., Yang, S.H., Meskini, A., 1990. A stiffness degradation model for graphite/epoxy laminates. *J. Compos. Mater.* 753–769.
- Yudhanto, A., Alfano, M., Lubineau, G., 2021. Surface preparation strategies in secondary bonded thermoset-based composite materials: A review. *Compos. Part A Appl. Sci. Manuf.* 147, 106443. <https://doi.org/10.1016/j.compositesa.2021.106443>.
- Zhang, Y., Vassilopoulos, A.P., Keller, T., 2010. Mixed-mode fracture of adhesively-bonded pultruded composite lap joints. *Eng. Fract. Mech.* 77, 2712–2726. <https://doi.org/10.1016/j.engfracmech.2010.06.017>.